Plant Stress 16 (2025) 100841

Contents lists available at ScienceDirect

Plant Stress

journal homepage: www.sciencedirect.com/journal/plant-stress

Lime-induced iron deficiency stimulates a stronger response in tolerant grapevine rootstocks compared to low iron availability

Sarhan Khalil [a,*], Rebeka Strah [b,c], Arianna Lodovici [d], Petr Vojta [e], Jörg Ziegler [f], Maruša Pompe Novak [b,g], Laura Zanin [d], Nicola Tomasi [d], Astrid Forneck [a], Michaela Griesser [a]

[a] Institute of Viticulture and Pomology, Department of Agricultural Sciences, University of Natural Resources and Life Sciences, Vienna, 3430 Tulln an der Donau, Austria
[b] Department of Biotechnology and Systems Biology, National Institute of Biology, 1000 Ljubljana, Slovenia
[c] Jožef Stefan International Postgraduate School, 1000 Ljubljana, Slovenia
[d] Department of Agricultural, Food, Environmental, and Animal Sciences, University of Udine, 33100 Udine, Italy
[e] Institute of Computational Biology, Department of Biotechnology and Food Science, University of Natural Resources and Life Sciences, 1190 Vienna, Austria
[f] Program Center MetaCom, Leibniz Institute of Plant Biochemistry, 06120 Halle Saale, Germany
[g] Faculty of Viticulture and Enology, University of Nova Gorica, 5271 Vipava, Slovenia

ARTICLE INFO

Keywords:
Vitis
Chlorosis
Fe deficiency
Bicarbonate
Ferric chelate reductase
RNA-seq

ABSTRACT

Iron (Fe) is abundant in soil, but its bioavailability can be limited by environmental factors, negatively impacting plant growth and productivity. While root mechanisms for enhancing Fe uptake are well-studied in some model plants, the responses of tolerant and susceptible grapevine rootstocks to low Fe availability remain poorly understood. This study examined the responses of two grapevine rootstocks, Fercal (tolerant) and 3309C (susceptible), to three Fe conditions: direct Fe deficiency (−Fe), induced Fe deficiency through the addition of bicarbonate (+Fe+BIC), and control (+Fe). Our main findings include: 1) more severe leaf symptoms in 3309C than in Fercal independent of the type of stress, 2) overall growth reduction due to direct Fe deficiency (−Fe), while under induced Fe deficiency (+Fe+BIC) Fercal strongly increased root biomass. This observation is supported by the increased expression of root-development related genes *VviSAUR66* and *VviZAT6,* 3) enhanced organic acid contents under induced Fe deficiency (+Fe+BIC) and different organic acids profiles depending on applied stress and genotype, and 4) stronger modulation of gene expression in Fercal root tips, including enhanced expression of Fe mobilization and transport genes (*VviOPT3, VviIREG3, VviZIF1*). Overall, bicarbonate-induced Fe deficiency (+Fe+BIC) had greater negative effects than direct Fe deficiency (−Fe), with Fercal showing a higher adaptive capability to maintain Fe homeostasis.

1. Introduction

Iron (Fe) deficiency is considered an important nutritional disorder in many crops and fruit trees, including grapevine (Bertamini and Nedunchezhian, 2005). Due to Fe role in various metabolic processes (e.g., respiration, chlorophyll formation, nitrogen assimilation, defense against oxidative stress and photosynthesis), any limitation in its availability negatively impacts plant development and health (Rout and Sahoo, 2015; Kobayashi et al., 2019). Initial symptoms appear on young leaves in the form of interveinal chlorosis finally affecting plant biomass production as the deficiency becomes more severe. (El Amine et al., 2023; Rustioni et al., 2017). The high pH of alkaline and calcareous soils is considered to be the main cause limiting bioavailability and solubility of Fe in cultivated soils (Tagliavini and Rombolà, 2001). Bicarbonate can cause chlorosis in plants via several mechanisms. Fe availability is reduced by high soil pH through the formation of insoluble Fe compounds (Saleem et al., 2023). In addition, bicarbonate ions can be transported into the plants, resulting in alkalization of the pH of the xylem sap, which can lead to inefficient Fe translocation (Lampreave et al., 2022). Furthermore, bicarbonate cause reactive oxygen species (ROS) to be produced (Valipour et al., 2020), and also negatively affects Fe homeostasis by downregulating the expression of those genes involved in ethylene biosynthesis and signaling, which in turn suppresses the activation of *Strategy I* Fe uptake genes, such as those encoding H^+-ATPase genes (*AHA1*), ferric chelate reductase (*FRO2*) and the Fe transporter (*IRT1*), leading to decreased Fe^{3+} reduction and

* Corresponding author.
E-mail address: sarhan.khalil@boku.ac.at (S. Khalil).

https://doi.org/10.1016/j.stress.2025.100841
Received 23 October 2024; Received in revised form 30 March 2025; Accepted 5 April 2025
Available online 6 April 2025

transport into root cells (Lucena et al., 2007).

In vineyards, foliar spraying with inorganic Fe salts (e.g., FeSO4) is the most effective method of treating Fe deficiency, but it is costly due to limited Fe penetration into the leaves and the need for repeated treatments (Chen and Barak, 1982; Yunta et al., 2013). Acid irrigation can also increase nutrient acquisition and lower soil pH to enhance Fe availability, although it is associated with environmental risks (Lampreave et al., 2022). The application of synthetic chelates such as Fe-EDDHA and Fe-EDDHMA is another widely used strategy to prevent Fe chlorosis, particularly in calcareous soils. However, despite their effectiveness, the high cost and the environmental risks associated with the use of these compounds highlight the requirement for sustainable alternatives (Tagliavini and Rombolà, 2001). Among these, planting lime-tolerant grapevine rootstocks such as Fercal (1B [Vitis Berlandieri x Ugni Blanc] x Richter 31) or 140 Ruggeri (V. Berlandieri x V. rupestris) seems to be the most effective and practical method to ensure adequate nutrient uptake and prevent Fe deficiency chlorosis in vineyards (Covarrubias and Rombolà, 2013, 2015; Vannozzi et al., 2017).

To improve Fe uptake, tolerant plants use different mechanisms to deal with low Fe bioavailability. When Fe availability is low, tolerant non-*graminaceous* plants can improve Fe acquisition by enhancing an acidification-reduction process known as *Strategy I* (Gao et al., 2019). Through this, specific isoforms of the plasma membrane H^+-ATPases, such as AHA2 actively pump protons (H^+), leading to rhizosphere acidification and increased Fe^{3+} solubility (Santi and Schmidt, 2009). Other H^+-ATPases isoforms, such as AHA7 may also contribute to Fe uptake regulation, though its role is less evident (Ivanov et al., 2012). Subsequently, Fe^{3+} (ferric form) is reduced to Fe^{2+} (ferrous one) by the enzyme ferric chelate reductase (FCR) in the root, which is encoded by *FRO* gene (Robinson et al., 1999), and finally *Iron-Regulated Transporter IRT* primarily transports Fe^{2+} into the root cells (Eide et al., 1996). In addition, tolerant plants can alter their root architecture under Fe deficiency by promoting the growth of root hairs and lateral roots (Młodzińska-Michta, 2023). Increasing root surface area may improve Fe acquisition by providing new sites for FCR activity (Challam et al., 2021).

A second pillar of the *Strategy I* plant response to low Fe availability is the increased biosynthesis of phenolics compounds and organic acids in the roots to enhance Fe acquisition via their exudation, which has been demonstrated for Fe, and also for other nutrients (Adeleke et al., 2017; Panchal et al., 2021; Abadía et al., 2002). Furthermore, organic acids anions released by plant roots such as malate into the rhizosphere can improve Fe solubility by forming complexes with Fe, making it more available for plant uptake (Justi et al., 2022; Molnár et al., 2023).

Previous studies, especially with annual species such as *Arabidopsis thaliana* (Kim et al., 2019), soybean (Atencio et al., 2021), rice (Aung et al., 2018), and maize (Li et al., 2014) showed that plants adapt their response to Fe deficiency depending on the cause of Fe deficiency and the plant genotype (Tao et al., 2020; Fu et al., 2017). In perennial crops, the specific knowledge is much more limiting. Early research primarily investigated the effects of Fe deficiency on plant growth, yield and fruit quality (Bavaresco et al., 1992; Belkhodja et al., 1998). as well as its impact on chlorophyll biosynthesis and photosynthetic efficiency (Bavaresco and Perino, 1994; Abadía, 1992). Subsequent studies highlighted the ability of certain genotypes to mitigate Fe deficiency damage, shedding light on their adaptive mechanisms under limited Fe availability. Tolerance to Fe deficiency has been linked to enhanced Fe acquisition strategies, including increased rhizosphere acidification (Abadía et al., 2002; Chen et al., 2017), enhanced ferric chelate reductase (FCR) activity (Molassiotis et al., 2005; Siminis and Stavrakakis, 2008; Pestana et al., 2012), and upregulation of Fe transporters (Martínez-Cuenca et al., 2013b). In recent years, focus has shifted toward molecular responses, with the identification of the responsive genes involved in Fe uptake and homeostasis (Masuda et al., 2018; Liang, 2022; Sun et al., 2022) However, a little is known about the molecular response mechanisms to Fe deficiency in grapevine roots, especially with different genetic backgrounds (Vannozzi et al., 2017; Khalil et al., 2024), and comparative studies on different sources of low Fe availability are lacking.

In this work, we have used two grapevine rootstocks that differ in the plant's response to Fe deficiency: Fercal (tolerant to Fe deficiency-induced chlorosis) and Couderc 3309 (3309C, highly susceptible to Fe deficiency-induced chlorosis). The differences in phenotype of these rootstocks' genotypes are described, but many aspects of their specific responses are still unknown. We investigated the peculiarities of plant response to two stress treatments leading to low Fe availability, namely no Fe supplied in the nutrient solution (−Fe) (causing direct Fe deficiency) and carbonate induced Fe deficiency (+Fe+BIC) (inducing Fe deficiency) compared to Fe-sufficient conditions (+Fe). Thereby, we aimed a) to characterize the responses at morphological, physiological, and transcriptional levels due to the applied stresses, and b) to extract the genotype-specific contribution to cope with the stress situations in order to identify possible processes explaining the described phenotypes. Our hypotheses state, that i) direct and indirect Fe deficiency address different response reaction in grapevine rootstocks, and that ii) the Fe translocation into shoots is reduced in susceptible rootstocks leading to more severe chlorosis symptoms. The research was performed with potted plants. Our results contribute to the knowledge gap of Fe uptake and translocation in grapevine.

2. Material and methods

2.1. Experimental design and plant material

The experiment was conducted in a glasshouse facility at BOKU University (Tulln, Austria) between April and June 2021. Woody cuttings from two grapevine rootstocks which have different tolerance to Fe deficiency were used: Fercal (1B [*Vitis Berlandieri* x Ugni Blanc] x Richter 31 [*Berlandieri Resseguiere 2* x *Novo Mexicana (interspecific cross V. riparia x V. rupestris x V. candicans)]*) as a lime-tolerant rootstock, and Couderc 3309 (*V. riparia* x *V. rupestris*) with a susceptibility to lime stress. The cuttings were rooted for six weeks in a combination of equal volumes of perlite and peat-clay substrate (1:1). The side shoots were removed. Rooted plants were transplanted individually into 3 L pots filled with fine quartz sand (0.5–2 mm) as substrate. The plants were manually watered daily with a modified half-strength Hoagland nutrient solution (Hoagland and Arnon, 1950, see details for nutrient solution composition at Khalil et al. 2024), starting with 100 mL and increasing to 300 mL following the plant growth. After a 10-day acclimation period for the plants to the new growing conditions, three treatments were started for 30 days: 1) Control (+Fe): 0 mM $KHCO_3$ + 50 µM NaFe (III)-EDTA; 2) Direct Fe deficiency (−Fe): 0 mM $KHCO_3$ + 0 µM NaFe(III)-EDTA; 3) Induced Fe deficiency (+Fe+BIC): 10 mM $KHCO_3$ + 50 µM NaFe (III)-EDTA. The concentration of Fe provided followed the recommendation of Covarrubias et al. (2016), with NaFeEDTA type used to mimic the low Fe availability and solubility in calcareous soils. The K concentration was not compensated in the control and −Fe treatment, as there was no option to add it as pure K. In addition, adding it in forms like K_2SO_4, KH_2PO_4, or KNO_3, would have altered sulfate, phosphate, or nitrate levels in the nutrient solution.

2.2. Analysis of morphometric parameters and evaluation of leaf chlorosis

At the end of the experiment, growth parameters such as shoot length (cm), growth rate (cm day^{-1}), leaf area (cm^2), and root and leaf biomass (FW (g) and DW (g) after 72 h at 80 °C) were measured on all plants ($N = 5$ each treatment and rootstock). Results for these data were obtained from old leaves (basal mature leaves, between the 5th and 10th insertion from the bottom of the shoot) and young leaves (fully developed leaf between 4th to 7th leaf insertion from shoot tip) were applicable. The Pouget index was used to monitor the development and severity of Fe chlorosis on the young leaves, as previously described (Pouget and

Ottenwaelter, 1978; Khalil et al., 2024).

2.3. Chlorophyll concentration

Photosynthetic pigments (total chlorophyll content (TotalChl), chlorophyll a (Chla), chlorophyll *b* (Chlb)) were determined at the end of the experiment by spectral photochemically method as previously described with minor modifications (Hiscox and Israelstam, 1979; Khalil et al., 2024). In brief, three leaf disks (1.8 cm in diameter, $N = 5$ from young and old leaves were freeze-dried for 48 h (Christ Beta 2–4 LD plus LT, Marin Christ Corporation, Osterode, Germany). Extraction was performed from 20 mg dried leaf tissue with 1.8 mL dimethyl sulfoxide (DMSO) at 40 °C for 45 min (Thermomixer comfort, Eppendorf, Hamburg, Germany). The colourless supernatant (1 mL) was obtained after centrifugation at 17000x*g* for 3 min at room temperature, and transferred to measure the absorbance at 645, 663, and 710 nm against DMSO as a blank. Concentrations were calculated as previously shown (Khalil et al., 2024).

2.4. Measurement of stomatal conductance and chlorophyll fluorescence

Leaf stomatal conductance (g_{sw}, mol m^{-2} s^{-1}) and leaf transpiration rate (E, mmol m^{-2} s^{-1}) was determined on sunny days (between 10 am – 2 pm) on mature fully expanded leaves ($N = 5$) using the LI-600 porometer (LI-COR Inc., Nebraska, USA) with a standardized light intensity of 10,000 µmol m^{-2} s^{-1} and ambient CO_2 concentration, leaf temperature and relative humidity. On the same leaves, the maximum quantum efficiency of PSII (Fv/Fm) after dark adaptation for 30 min was measured with the Plant Efficiency Analyzer (PEA, Hansatech Instruments Ltd., UK)

2.5. Root ferric chelate reductase (FCR) activity

The FCR activity quantification followed a protocol described in Marastoni et al. (2020). In short, apical root tips (100 mg) were first transferred to 2 mL of 0.2 mM $CaSO_4$ for 10 min at room temperature, before transferred for 1 h incubation in the dark to 2 mL of the assay solution (5 mM MES-NaOH (pH 5.5), 10 mM $CaSO_4$, 0.1 mM Fe (III)-EDTA, and 0.3 mM sodium bathophenanthroline disulfonic acid (Na-BPDS) (all chemicals from Merck KGaA, Darmstadt, Germany). Absorbance was measured in 1 mL at 535 nm (Spectrophotometer Genesys, Thermo Fisher Scientific) against BPDS as a blank after 2 min centrifugation at max. speed at room temperature. Enzyme activity is calculated as recently described (Khalil et al., 2024).

2.6. Organic acids' concentration in root tips and root exudates

Organic acids in root tips were quantified as described by Savoi et al. (2019) from 20 mg of freeze-dried plant material. Root exudates collection followed the protocol described by Santangeli et al. (2024). The whole root apparatus of four intact plants per treatment were rinsed and then soaked in ddH_2O in plastic vessels for 5 min (repeated three times). The roots were then transferred to 400 mL ddH_2O containing 10 mg L^{-1} Micropur (Katadyn, Zurich, Switzerland) to prevent the growth and activity of microorganisms and covered with aluminium foil to prevent light exposure. After two hours of exudate sampling, the roots were removed and 50 mL of each sample was filtered into 50-mL tubes using 0.2 µm PES-20/25 syringe filters (Chromafil® Xtra, Macherey-Nagel, Germany) and then stored at −80 °C. 200 µl of the root exudate was analyzed for organic acid content as recently described (Chutia et al., 2021).

2.7. Elemental analyses in plant tissues

Following a protocol by Zanin et al. (2017), the concentrations of macro- and micronutrients were determined using Inductively Coupled Plasma–Optical Emission Spectroscopy (ICP-OES 5800, Agilent Technologies, Santa Clara, USA) and a CHN analyzer (CHN IRMS Isoprime 100 Stable Isotope Ratio Mass Spectrometer, Elementar, Como, Italy). For ICP analyses, plant material was ground after drying for 72 h at 80 °C before incineration of 100 mg at 550 °C and afterwards suspension in 10 mL of ultrapure HNO_3. Quantification occurred using certified multi-element standards. For CHN analyses, 2–4 mg of the dried ground powder of each sample was analysed using the CHN analyzer.

2.8. RNA extraction, RNA-Seq analysis, and bioinformatics

Root tips collected at the end of the experiment (three biological replicates representing three independent plants grown separately in their own pots under the same conditions per treatment) were ground in liquid nitrogen and 100 mg were used for total RNA extraction with the Spectrum Plant Total RNA Kit (Merck KGaA, Darmstadt, Germany).

In total 18 samples were used for RNA-Seq, which was conducted as a commercial service with Novogene Europe (Novogene, Cambridge, UK) as paired-end 150-bp sequencing on an Illumina platform NovaSeq 6000. STAR aligner (Dobin et al., 2013) was used for fastq sequences to align to the reference genome, while quality checks were performed with FastQC, Qualimap, and MultiQC (Simons, 2010; Okonechnikov et al., 2016; Ewels et al., 2016) and recently descibed by Khalil et al. (2024).

The grapevine reference genome PN40024.v4 was obtained from the INTEGRAPE website as general feature format (GFF) (https://integrape.eu/resources/genes-genomes/genome-accessions/) and a functional gene annotation was performed using the BLAST2GO (Götz et al., 2008). Count data per gene was obtained with featureCounts (Liao et al., 2014).

Genes with a False Discovery Rate (FDR) threshold of less than 0.05 and absolute fold change greater or equal to 1.0 were defined as differently expressed genes (DEGs) between the compared groups. The integrated Differential Expression and Pathway analysis tool (iDEP 2.0) (Ge et al., 2018) was used for GO (gene ontology) enrichment analysis. Selected enriched biological processes were plotted using an adapted protocol as described in Bonnot et al. (2019), within the ggplot2 package (v3.5.0) in R (v4.2.3; https://www.R-project.org/). In addition, principal component analysis (PCA) was performed using DESeq2 (v1.8.3) (Love et al., 2014) and visualized using the same ggplot2 package.

2.9. Statistical analyses

Statistical analyses were performed by using IBM SPSS statistic software (IBM Corp. IBM SPSS Statistics for Windows, Version 27.0. Released 2020. Armonk). While OriginPro software (Seifert, 2014), SRPLOT online tool (https://www.bioinformatics.com.cn/en) and RStudio (v2024.04.0; +544) were used to generate graphs.

3. Results

3.1. Plant growth and leaf performance

In both tested rootstocks, a limitation of shoot growth was observed under low Fe availability (Table 1). Compared to the control condition (+Fe), induced (+Fe+BIC) Fe deficiency significantly reduced plant growth by 39 % in 3309C and 41 % in Fercal. In contrast, direct Fe deficiency (−Fe) caused minimal growth reduction in Fercal (8 %) and a moderate reduction in 3309C (29 %). Young leaf development was affected by the two applied treatments, with a reduction in leaf area in Fercal (42 % and 46 % under −Fe and +Fe+BIC, respectively) and 3309C (51 % and 61 % under −Fe and +Fe+BIC, respectively) (Fig. 1B). Leaf chlorosis symptoms followed the growth pattern, with the most severe symptoms observed with young leaves of 3309C (Fig. 1A). These visual results were confirmed by the analyzed leaf chlorophyll concentration (Fig. 1C). The highest total chlorophyll concentration (6.84 mg. g^{-1}) was determined in young leaves of 3309C under control condition

Table 1
Parameters to assess plant growth and physiology. Mean values and standard deviations within rootstocks (3309C and Fercal) and treatments (+Fe, −Fe, and +Fe+BIC). Significant differences are indicated by different letters between treatments within each rootstock ($\alpha < 0.05$, One-way ANOVA and Tukey post hoc test, $N = 5$).

Genotype	Treatment	Growth rate (cm d^{-1})	Leaves dry weight (g)	Root dry weight (g)	Root/shoot Ratio	Stomatal conductance (mol m^{-2} s^{-1})	Transpiration rate (mmol m^{-2} s^{-1})	Fv/Fm
3309C	+Fe	4.19 ± 0.41 a	4.57 ± 1.24 a	1.27 ± 0.48 a	0.08 ± 0.02 b	0.40 ± 0.04 a	9.06 ± 1.05 a	0.82 ± 0.01 a
	−Fe	2.99 ± 1.21 ab	2.46 ± 0.98 b	1.37 ± 0.36 a	0.12 ± 0.05 b	0.29 ± 0.20 a	6.45 ± 2.53 a	0.80 ± 0.01 a
	+Fe+BIC	2.58 ± 0.69 b	1.71 ± 1.36 b	2.05 ± 1.31 a	0.20 ± 0.05 a	0.27 ± 0.06 a	7.47 ± 2.84 a	0.77 ± 0.05 b
Fercal	+Fe	4.49 ± 0.67 a	7.32 ± 2.37 a	2.73 ± 1.20 b	0.18 ± 0.08 b	0.42 ± 0.11 a	9.17 ± 2.30 a	0.81 ± 0.02 a
	−Fe	4.14 ± 1.37 ab	4.30 ± 1.29 a	2.70 ± 1.50 b	0.22 ± 0.05 b	0.36 ± 0.19 a	8.05 ± 3.55 a	0.80 ± 0.01 a
	+Fe+BIC	2.68 ± 0.68 b	4.74 ± 0.89 a	6.62 ± 1.25 a	0.42 ± 0.04 a	0.35 ± 0.13 a	9.16 ± 2.21 a	0.78 ± 0.04 a

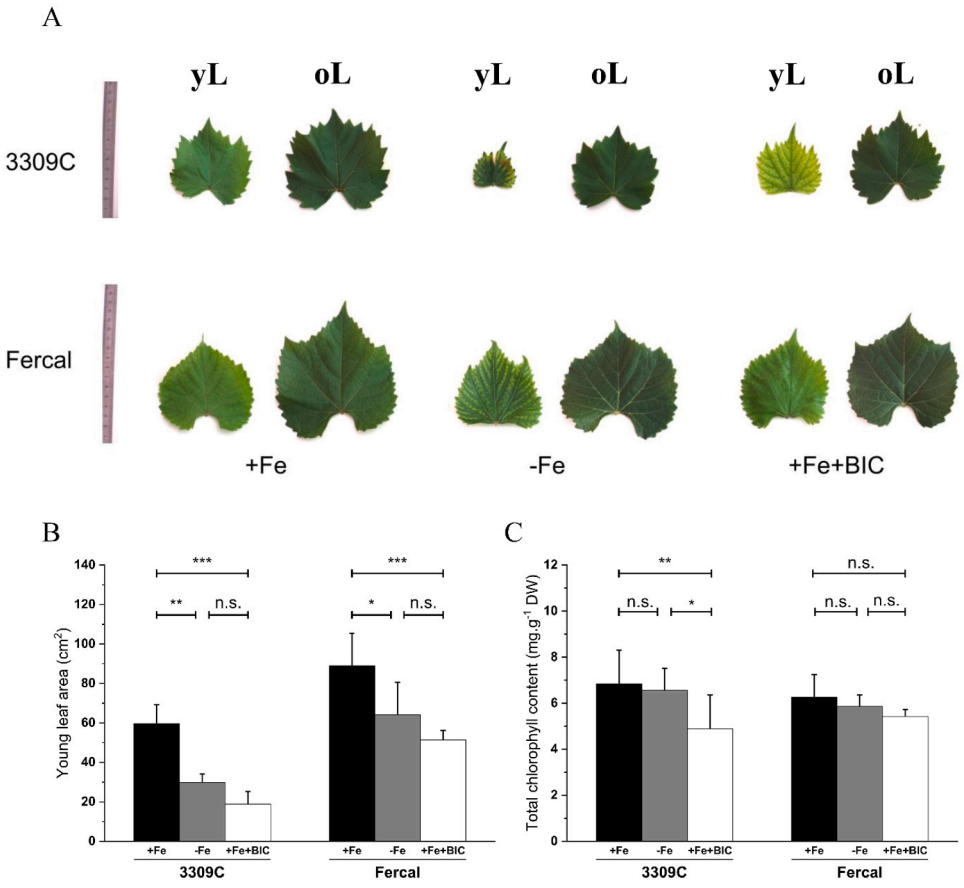

Fig. 1. Parameters obtained with leaves after 30 days for rootstocks 3309C and Fercal and all treatments (+Fe; −Fe; +Fe+BIC)**.** A) 3309C and Fercal young and old leaves phenotype, B) young leaf area (cm^2), and C), total chlorophyll concentration in young leaves (mg g^{-1} DW). Values shown as means ± SD ($N = 5$). Asterisks (*, ** and ***: $p < 0.05$, 0.01, and 0.001, respectively) and indicate significant differences between treatments within each rootstock n.s. denotes not significant (Tukey's HSD).

(+Fe). However, this value was significantly reduced to 4.88 mg. g^{-1} in 3309C with +Fe+BIC treatment. In Fercal a strong negative effect of +Fe+BIC treatment was not observed, with chlorophyll levels measuring 5.42 mg. g^{-1} compared to 6.26 mg. g^{-1} in the control) (Fig. 1C). Although growth of young leaves was affected, the stress treatments did not influence neither the photosynthetic efficiency of the photosystem II of dark-adapted leaves (Fv/Fm), nor the stomatal conductance (g_{sw}) nor the transpiration rate (E) of light-exposed young leaves (Table 1).

3.2. Root development and ferric chelate reductase enzyme activity

The root DW increased by 60 % ($P < 0.05$) and 142 % ($P < 0.001$) in 3309C and Fercal under +Fe+BIC compared to +Fe, respectively (Fig. 2A, B). The −Fe treatment had no impact on root biomass compared to the +Fe condition in both rootstocks. The root:shoot biomass ratio (Table 1) was enhanced in Fercal as well as in 3309C, but the mechanism seems to be different. Fercal strongly enhance root growth under carbonate stress, the root system in 3309C was not

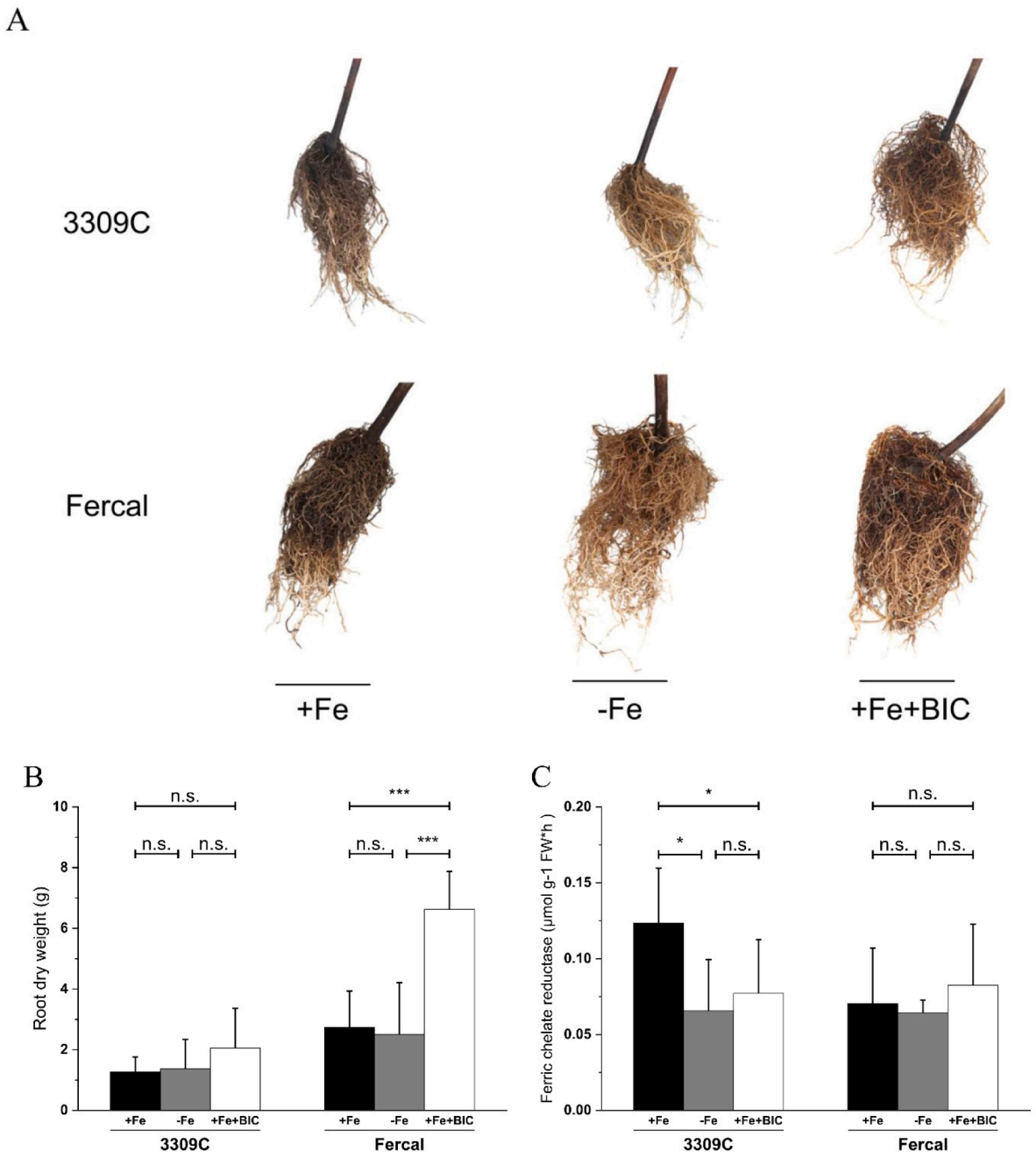

Fig. 2. Root growth and Fe chelate reductase activity of both rootstocks at different treatments (+Fe; −Fe; +Fe+BIC). A) phenotype of the root systems of both rootstocks, B) root dry weight (g), and (C) FCR activity in root tips (µmol g^{-1} FW h^{-1}). Values shown as means ± SD ($N = 5$). Asterisks (*, ** and ***: $p < 0.05$, 0.01, and 0.001, respectively) indicate significant differences between treatments within each rootstock and ns denotes not significant (Tukey's HSD).

affected while plant growth was reduced.

Activity of FCR enzyme was tested at the end of the experiment (30 days after treatment) in the collected root tips (Fig. 2C). This long-term response yielded some surprising results, 3309C (the susceptible rootstock) had the highest FCR activity in control roots and showed a significant drop in FCR activity under both Fe deficiency conditions compared to +Fe. Interestingly, this drop in FCR activity was not determined in the roots of Fercal (the tolerant rootstock), where no significantly different results were observed between treatments.

3.3. Organic acids in root tips and root exudates

The concentration of organic acids in the root tips tended to increase under Fe deficiency conditions, especially under +Fe+BIC treatment in both rootstocks (Fig. 3A-C). Malic acid concentration in Fercal root tips was significantly higher under −Fe (100 %) and +Fe+BIC treatments (300 %) compared to +Fe, while no increase was observed in 3309C root tips under direct (−Fe) Fe deficiency and an increase of (100 %) under induced (+Fe+BIC) Fe deficiency. The results obtained for citric and tartaric acid concentration in root tips were not conclusive due to high variability among tested samples, and the response of the rootstocks was not homogeneous. The content of organic acids in root exudates gave different results than in the root tips (Fig. 3D-F). A significant increase in malic and tartaric acid concentration was determined in 3309C under −Fe treatment (730 % and 530 %, respectively), while citric acid was enhanced by (530 %) under the same treatment in Fercal (Fig. 3D, E). Treatment with bicarbonate resulted in higher amount of citric acid and tartaric acid in both rootstocks, although not all results were determined

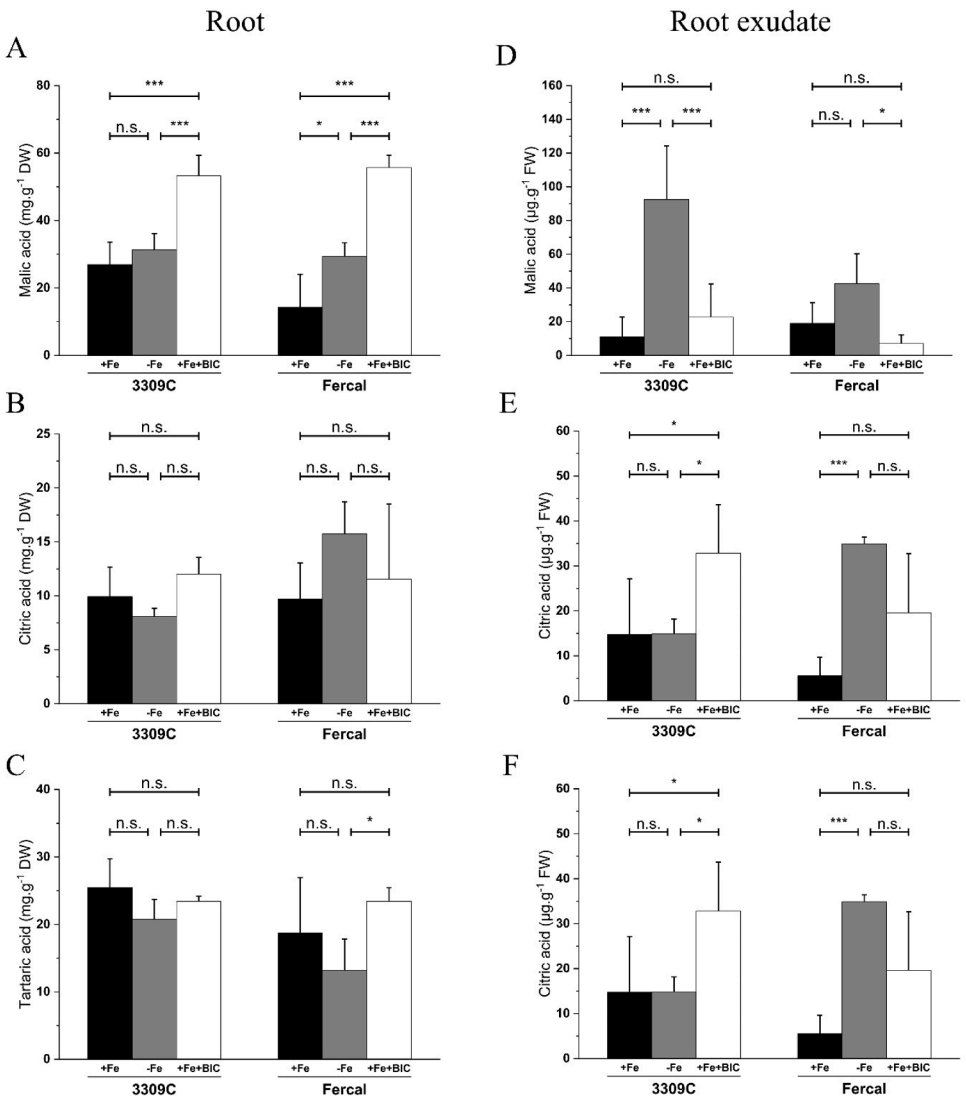

Fig. 3. Organic acids' concentration (A-C) in root tips and (D-F) in root exudates after 30 days of different treatments (+Fe; −Fe; +Fe+BIC). Values shown as means ± SD ($N = 3$). Asterisks (*, ** and ***: $p < 0.05$, 0.01, and 0.001, respectively) indicate significant differences between treatments for each rootstock and ns denotes not significant (Tukey's HSD).

as significantly different ($p < 0.05$) compared to +Fe (Fig. 3E, F). In particular, the results of malic acid (Fig. 3A, D) indicate that malic acid is produced under +Fe+BIC in both rootstocks but is not released into the root exudates, whereas under −Fe the release tends to be higher for all organic acids.

3.4. Iron and other nutrients' content

Although Fe concentration, in both young and old leaves, was not significantly affected by any Fe deficiency treatments (Fig. 4A, B), symptoms were observed in young leaves (Fig. 1A). In contrast to the results in the leaves, Fe content in the roots was strongly reduced by Fe deficiency treatments in both rootstocks (Fig. 4C). In 3309C, the −Fe treatment reduced the concentration in roots by 73 %, while the reduction by 37 % was less evident under induced (+Fe+BIC) Fe deficiency. In the Fercal rootstock, both Fe deficiency treatments lead to lower amounts of Fe in roots with a reduction of 65 %. Surprisingly, the Fe content in the roots was higher in the control plants (+Fe) of 3309C compared to Fercal. This was also observed in the leaves, although the differences were not statistically significant ($p < 0.05$). Based on these analytical results, the distribution ratio of Fe between the analyzed organs was calculated (Fig. 4D). Regardless of the Fe concentration, both rootstocks showed similar Fe distribution ratios in all analyzed plant parts under +Fe and −Fe treatments. In contrast, with +Fe+BIC treatment the ratio in 3309C was very similar to the results for the corresponding control plants, while the ratio in Fercal +Fe+BIC resembled the calculated values for −Fe treatments (Fig. 4D). Moreover, Fe deficiency treatments altered the concentration of several macro- and micronutrients (P, K, Ca, Zn, and Mn) in the analyzed plant tissues (Table S1). In young leaves: P concentration was increased by −Fe treatment, with a more pronounced increase in Fercal than in 3309C. However, P decreased by 46 % in the young leaves of 3309C under +Fe+BIC treatment. Potassium content was increased in both Fe deficiency treatments with a stronger increase observed under +Fe+BIC treatment. Content of Mn was strongly reduced by 54 % under +Fe+BIC treatment in both rootstocks, but increased under −Fe treatment (30 % in 3309C and 79 % in Fercal). In roots, bicarbonate stress (+Fe+BIC) had a stronger impact than −Fe treatment, reducing P and Mn concentrations significantly, with Fercal roots showing a higher reduction compared to 3309C. Similar to the results in leaves, the K concentration was enhanced in both Fe deficiency treatments, especially under +Fe+BIC treatment. In −Fe treatment only Fercal roots had decreased values for Ca and Zn concentration as compared to +Fe.

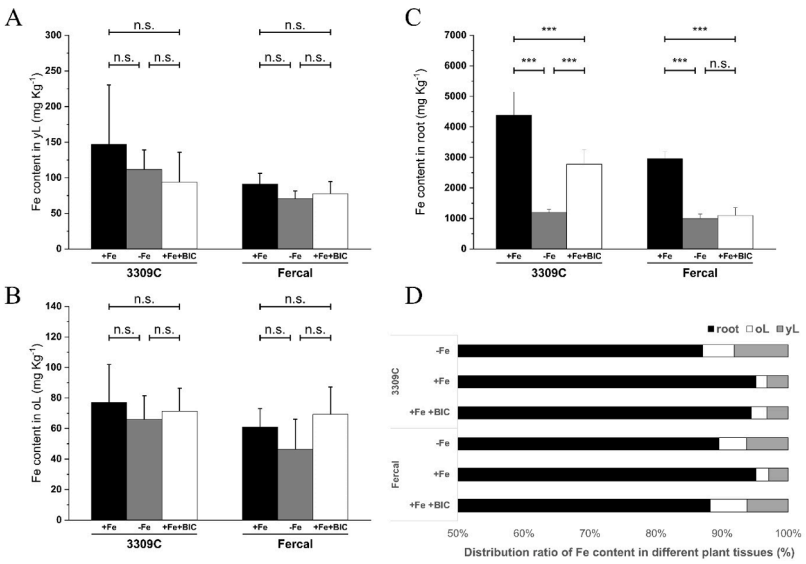

Fig. 4. Iron content in (A) young leaves, (B) old leaves, (C) root, and (D) Fe distribution ratio in plant tissues of either grapevine rootstocks, 3309C, or Fercal grown at different treatments (+Fe; −Fe; +Fe+BIC). Values are means ± SD; Mean values with the same letters within the same rootstock and same plant tissue are not significantly different rootstock (*, ** and ***: $p < 0.05$, 0.01, and 0.001, respectively, and ns denotes not significant (Tukey's HSD).

3.5. Transcriptional profiling reveals changes in gene expression as a response to Fe deficiency treatments

Raw reads from a RNASeq study of root tips ranged from 39.47 to 46.73 million reads, of which more than 97 % were identified as clean reads, resulting in 38.34 to 45.64 million clean reads. The average GC content was around 45 % for all libraries, and the Q20 and Q30 scores of clean reads were above 97 % and 93 %, respectively (Table S2). PCA analysis confirmed good clustering of the three biological replicates within each applied treatment and separation of the treatments along the PC2 axis, particularly of +Fe+BIC from the other two treatments (Fig. 5B). In addition, the analysis showed a clear separation between Fercal and 3309C rootstocks along the PC1 axis, which represented 70 % of the variance.

115 and 284 differentially expressed genes (DEGs) were indicated in the comparison of −Fe with +Fe in 3309C and Fercal, respectively. The number of DEGs in the comparison for of +Fe+BIC with +Fe were 2731 and 4370 DEGs for 3309C and Fercal. Genes commonly regulated between both Fe deficiency treatments were 47 DEGs (33 up-regulated and 14 down-regulated) for 3309C and 71 DEGs (25 up-regulated and 46 down-regulated) for Fercal (Fig. 5A). The known function of the commonly up- and downregulated genes through these comparisons are provided in the supplementary material (Tables S7 – S10).

Gene Ontology (GO) analysis was applied and the enriched genes in were annotated into two GO categories: biological process (BP) and molecular functions (MF) (Tables S3 - S6). Among them, only the biological process GO terms most significantly enriched for DEGs are shown in Fig. 6A, B. The most relevant biological processes associated with up-regulated DEGs in Fercal under Fe deficiency conditions (−Fe vs +Fe) were ion transport, transmembrane transport, and a slight increase in carbohydrate transmembrane transport. While, in 3309C, the categories transmembrane transport, ion transmembrane transport, ion transport, inorganic ion transmembrane transport, and phosphate ion transport were enriched. Categories enriched with down-regulated DEGs were metal ion transport in Fercal and response to temperature stimulus, response to hydrogen peroxide, and fatty acid catabolic process in 3309C (Fig. 6A).

The comparison of +Fe+BIC vs +Fe showed a higher number of DEGs in both rootstocks, resulting in a higher number of GO subcategories. (Fig. 6B). In Fercal, up-regulated DEGs were significantly enriched for the catabolic process, generation of precursor metabolites and energy, organic acid metabolic process, and response to abiotic

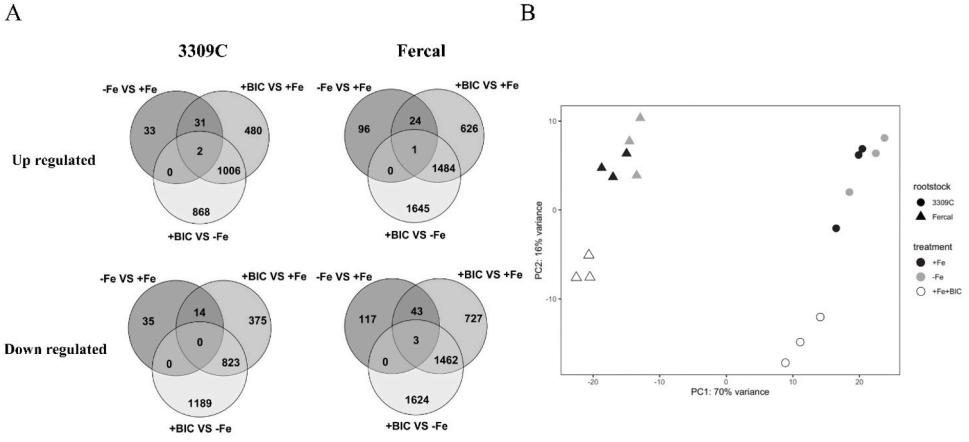

Fig. 5. Differentially expressed genes. (A) Venn diagram of DEGs ($|\log_2 FC| \geq 1$) in both rootstocks and (B) Principal Component Analysis (PCA) of top enriched genes. Circles represent 3309C genotype, and triangles represent Fercal genotype, while the treatments are represented in different colors.

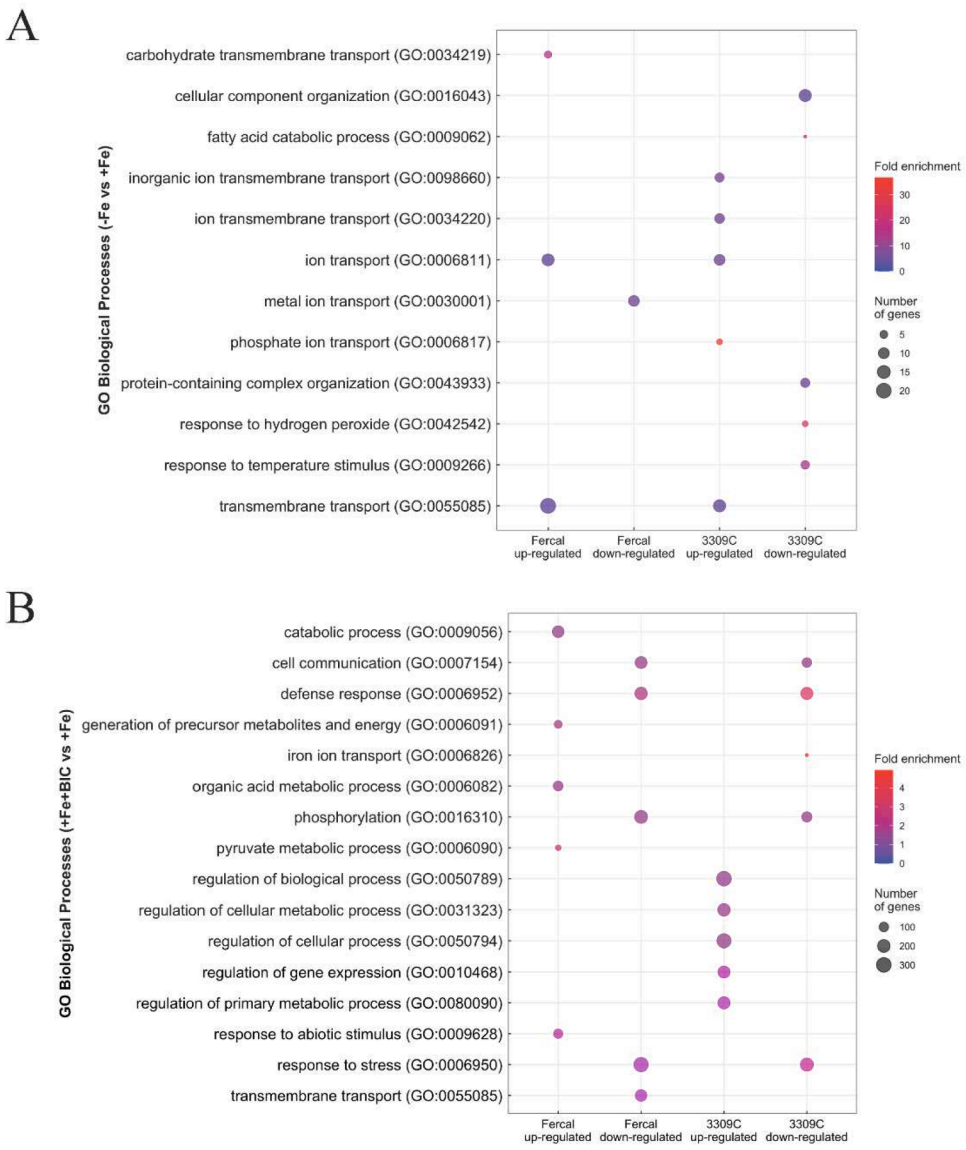

Fig. 6. Functional and Enrichment pathways of DEGs. Top enriched GO terms of biological process (BP) in Fercal and 3309C in, (A) (−Fe vs +Fe) comparison and (B) (+Fe+BIC vs +Fe) comparison. Fold enrichment is represented by colored dots while dot size reflects the number of genes involved in each pathway.

stimulus. In 3309C, biological processes associated with the regulation of cellular metabolic process and regulation of biological process were enriched by up-regulated DEGs. In contrast, many down-regulated DEGs were commonly enriched in both genotypes in several biological processes, such as defense response, and cell communication.

3.6. Iron deficiency conditions lead to altered expression of genes involved in Fe homeostasis and root development

To better understand the Fe-related genes affected by direct (−Fe) and induced (+Fe+BIC) Fe deficiency in both grapevine rootstock genotypes, we investigated the expression patterns of genes known to be involved in Fe uptake, transport, storage, homeostasis, root development and organic acid (Fig. 7). The common and uncommon responses of the studied genes to ferrome, in relation to Fe uptake, transport and root development in our grapevine rootstocks under Fe deficiency are presented in (Table S11).

Genes involved in Fe acquisition by *Strategy I* plants (*VviAHA2, VviFRO2, VviIRT1*) were not strongly affected, except of *Iron-Regulated Transporter 1* (*VviIRT1*), which was strongly up-regulated in 3309C (Log_2FC: 2.5 and 4.8 between −Fe and +Fe, and +Fe+BIC and +Fe, respectively) and slightly up-regulated in Fercal (Log_2FC: 1.4 and 1.2 between −Fe and +Fe, and +Fe+BIC and +Fe, respectively). Fe homeostasis regulators (*VvibHLH38, VvibHLH38/39*) were induced in both rootstocks, with stronger activation in 3309C under +Fe+BIC and in Fercal under −Fe. For Fe transport and translocation, most genes (*VviVIT1, VviIREG3, VviOPT3, VviNRAMP1, VviYSL6*) showed limited expression changes, though levels were generally lower in 3309C. Exceptions include *VviFRD3 and VviNRAMP6,* which were highly expressed under both stress conditions, which 3309C showing higher expression under +Fe+BIC and Fercal under −Fe. In addition, *VviZIF1* expression increased under −Fe in both rootstocks but only in Fercal under +Fe+BIC. The expression of the Fe storage gene *FERRITIN1* (*VviFER1*) decreased under −Fe in both rootstocks, but responses to +Fe+BIC differed, with 3309C showing reduced expression and Fercal showing no change.

Enhanced root growth and development in response to Fe deficiency was reflected in gene expression. *VviZAT11* gene expression was increased in both rootstocks by +Fe+BIC treatment, while *VviZAT6* was uniquely increased in Fercal under +Fe+BIC. Moreover, Auxin-responsive genes (*VviSAUR, VviSAUR66)* strongly increased under +Fe+BIC treatment in both rootstocks, but especially in Fercal. The

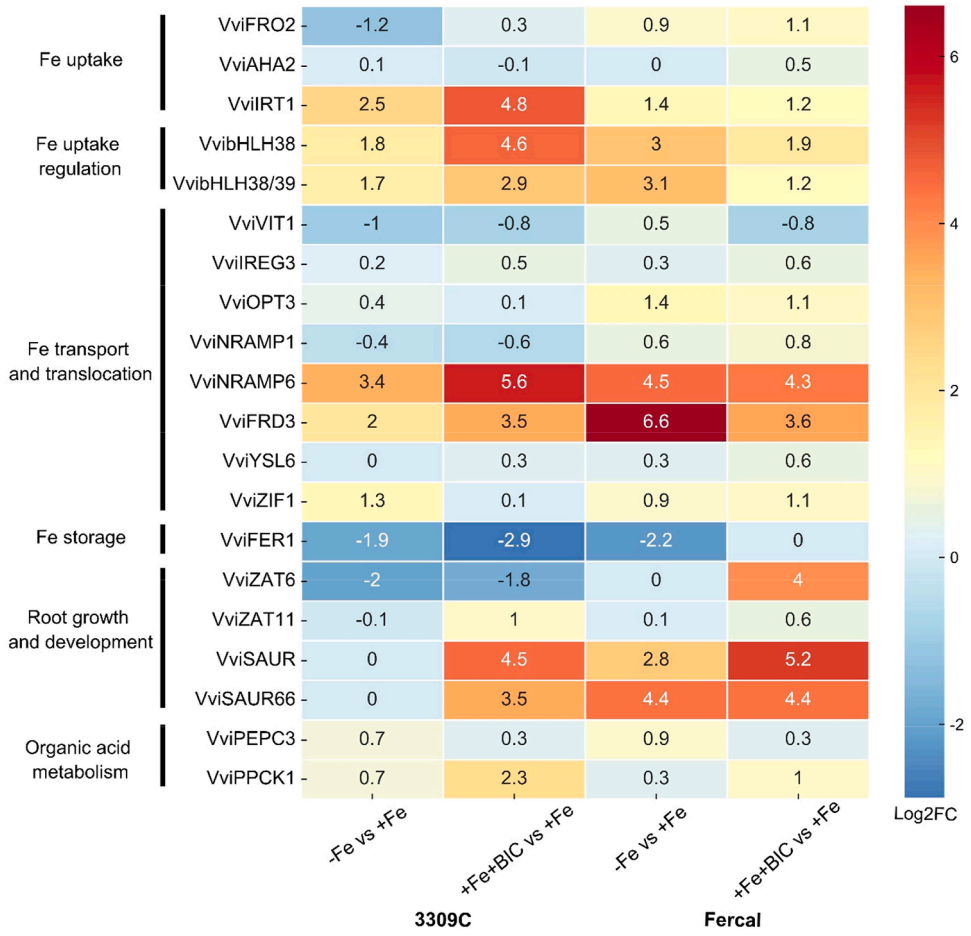

Fig. 7. Heatmap of Gene Expression of Differently Expressed Genes (DEGs). Change in expression (log_2FC) of several genes involved in Fe uptake (***VviFRO2*** *(Vitvi16g01090);* ***VviAHA2*** *(Vitvi11g01208);* ***VviIRT1*** *(Vitvi10g01356)*); Fe transport and translocation (***VviVIT1*** *(Vitvi15g00758);* ***VviOPT3*** *(Vitvi10g00247);* ***VviIREG3*** *(Vitvi14g00086);* ***VviNRAMP1*** *(Vitvi18g00242);* ***VviNRAMP6*** *(Vitvi18g00241);* ***VviYSL6*** *(Vitvi14g01520);* ***VviFDR3*** *(Vitvi13g01734);* ***VviZIF1*** *(Vitvi13g01095)*); Fe deficiency regulation (***VvibHLH38*** *(Vitvi13g01164);* ***VvibHLH38/39*** *(Vitvi08g01649)*); Fe storage (***VviFER1*** *(Vitvi08g00761)*) and root development (***VviZAT6*** *(Vitvi05g00082);* ***VviZAT11*** *(Vitvi06g01682);* ***VviSAUR*** *(Vitvi03g01471);* ***VviSAUR66*** *(Vitvi03g01458)*); and organic acids metabolism (***VviPEPC3*** *(Vitvi12g00185*); ***VviPPCK1*** *(Vitvi05g00736)*) in both rootstocks between both Fe deficiency treatments and control; no Fe available vs control (−Fe vs +Fe) and Bicarbonate stress vs control (+Fe+BIC vs +Fe). Values represent the log_2FC, where blue is the higher expression and yellow lower expression.

same genes were also induced under −Fe treatment only in Fercal.

Organic acids metabolism genes showed varied expression. Our data showed an increased expression of *Phosphoenolpyruvate carboxylase 3* (*VviPEPC3; VviPPC3*) under both Fe deficiency conditions, particularly under −Fe, while the expression of *Phosphoenolpyruvate carboxylase kinase 1* (*VviPPCK1*), regulating PEPC activity, was more strongly expressed under bicarbonate stress in both rootstocks

3.7. Iron deficiency stresses enhance the metabolic pathway of organic acids

Both Fe deficiency treatments induced changes in the content of malate and citrate in roots and root exudates. To better understand the changes leading to this outcome, we examined the changes in expression of genes involved in the TCA (tricarboxylic acid) cycle in roots (Fig. 8). Overall, the fold changes were not large, and few of the changes were statistically significant, which is consistent with the strong post transcriptional regulation of the enzymes involved in the TCA. Furthermore, both rootstocks appeared to respond similarly to both treatments. The most noticeable changes were in genes coding for pyruvate dehydrogenase, aconitase, isocitrate dehydrogenase, α-ketoglutarate dehydrogenase, fumarase, and malate dehydrogenase. Direct Fe deficiency (−Fe) induced a down-regulation for both rootstocks, while induced Fe deficiency (+Fe+BIC) induced an up-regulation. These changes are largest for α-ketoglutarate dehydrogenase and malate dehydrogenase, both enzymes which provide reducing equivalents for the cell in the form of NADH. The changes in gene expression could not be directly correlated with the changes of organic acids observed in roots and root exudates, however, the accumulation of malate in roots exhibited a similar pattern of change, increasing significantly under induced Fe deficiency (+Fe+BIC).

4. Discussion

It is evident, that grapevine rootstocks differ in their ability to cope with high lime contents in soils and prevent leaf chlorosis of scions. These studies led to a ranking of rootstocks from susceptible to tolerant. In perennial plants including grapevine, the mechanisms behind these observed phenotypes are not well understood, especially not on the molecular or biochemical level. Our study contributes to close this knowledge gap and aims to answer some open questions in the mechanistic response of rootstock genotypes to different sources of Fe deficiency. A summary of our key results in presented in Table 2.

4.1. Strong growth response and severe chlorosis upon Fe deficiency with still high Fe levels in leaves

In agreement with previous studies (Al-Mansouri and Alhendawi,

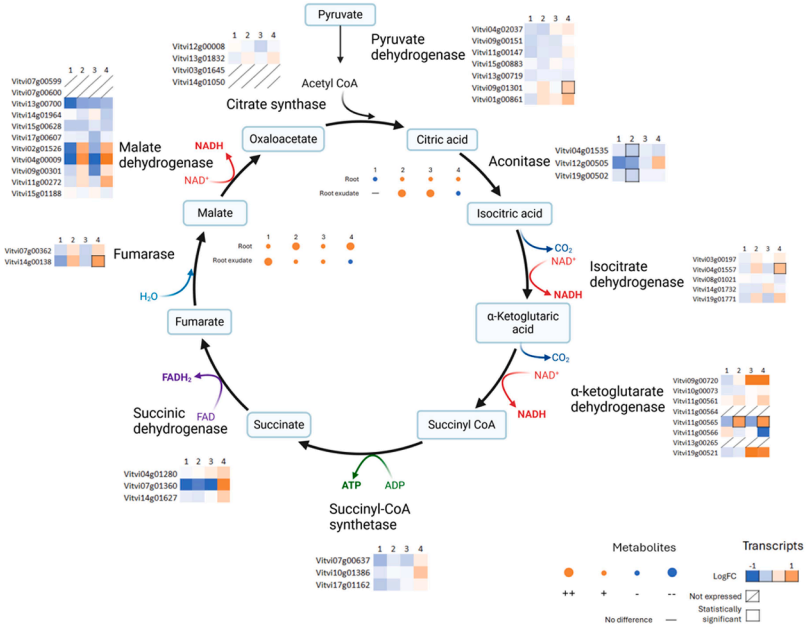

Fig. 8. Log_2FC changes in expression of genes involved in TCA cycle. Treatments: 1: 3309C no Fe available vs control (−Fe vs +Fe); 2: 3309C bicarbonate stress vs control (+Fe+BIC vs +Fe); 3: Fercal no Fe available vs control (−Fe vs +Fe); 4: Fercal bicarbonate stress vs control (+Fe+BIC vs +Fe).

Table 2
Summarized key results differentiating genotype and treatment specific responses. (+) enhanced, (−) decreased, (~) no response of grapevine plants under both Fe deficiency treatments (−Fe and +Fe+BIC) compared to the control (+Fe).

	3309C		Fercal	
	−Fe	+Fe+BIC	−Fe	+Fe+BIC
Shoot growth	− −	− − −	− −	− − (−)
Root growth	~	+	~	+ + +
Symptoms	+ +	+ + +	+	+ +
FCR activity	−	−	~	+
OA – malate roots	~	+ +	+	+ + +
OA – malate exudates	+ + +	~	+	~
OA – citrate roots	~	~	+	~
OA – citrate exudates	~	+	+ + +	+
Fe conc. roots	− − −	− −	− − −	− − −
Fe conc. leaves	~ −	~ −	~	~
DEGs	+	+ +	+ (+)	+ + +
Fe uptake (*VviIRT1*)	+ +	+ + +	+	+
Regulation (bHLH genes)	+	+ + +	+ + (+)	+
Fe transl. (*VviNRAMP6, VviFRD3*)	+ +	+ + +	+ + +	+ + (+)
Fe storage (*VviFER1*)	− −	− −	− −	~
Root growth (*VviZAT6*)	− −	− −	~	+ + (+)
Root develop. (SAUR genes)	~	+ + (+)	+ + (+)	+ + +
Organic acids (*VviPPCK1*)	+	+ +	~	+

2014; Sabir et al., 2010; Wang et al., 2022), our data confirmed growth depression in both tested grapevine rootstocks growing under both Fe deficiency treatments as a result of low Fe availability. Although Fe concentration was not significantly reduced in young apical and older basal leaves in our study (Fig. 4A, Table 2), the consequences on chlorophyll concentration and observed chlorosis symptoms were severe in the susceptible rootstock 3309C, especially under induced (+Fe+BIC) Fe deficiency. This phenomenon, known as "Fe chlorosis paradox," has been attributed to the possibility that chlorosis is caused by Fe inactivation in these leaves (Bavaresco et al., 1999; Römheld, 2000). The tolerant rootstock Fercal seems to maintain higher Fe and chlorophyll contents in young leaves under Fe deficiency conditions, aligning with similar findings observed in the 140Ru tolerant rootstock as reported by Ksouri et al. (2006). The stronger effect observed under +Fe+BIC especially in the susceptible rootstock 3309C could support the hypothesis of immobilization of Fe within the plant due to high bicarbonate affecting pH homeostasis within plant tissues (Tato et al., 2020; Römheld, 2000). Whereas another study suggested that different grapevine cultivars have different priorities in the utilization of Fe in young leaves under bicarbonate stress, either in chlorophyll biosynthesis or in limiting oxidative damage through the activation of enzymes that scavenge reactive oxygen species (ROS) (Karimi and Salimi, 2021). However, further studies are needed to clarify the priority of Fe utilization by stressed leaves in the case of tolerant and susceptible grapevine rootstocks.

Previous studies confirmed a genotype dependence of chlorosis symptoms in grapevine (Vannozzi et al., 2017; Covarrubias and Rombolà, 2013) and other fruit trees (Donnini et al., 2009; Asins et al., 2020), but we could additionally show a dependence of chlorosis severity on the cause of Fe shortage (Fig. 1A). Although symptoms were severe, the stomatal conductance (g_{sw}) or the transpiration rate (E) of the leaves were not severely affected in our study. Such changes in the photosynthetic activity of the plant have been observed in previous study (Covarrubias et al., 2016; Khalil et al., 2024), while we observed only a minor reduction in Fv/Fm values compared to +Fe leaves with chlorotic leaves of Fe deficiency 3309C under bicarbonate stress. This observed reduction is due the negative effect of bicarbonate on the transport of electrons and energy of PSII (Sun et al., 2022; Bertamini et al., 2001). In summary this indicates that leaves were able to keep stomata open, while the efficiency of photosynthesis was reduced to due oxidative stress damage.

Apart from Fe, other minerals may also have contributed to the observed leaf symptoms in dependence of the source of Fe limitation. Treatment without Fe led to higher concentration of P, K, Ca, and Mn in young apical leaves, while the treatment with +Fe+BIC resulted in a significant decrease in P and Mn concentrations Similar responses have already been described in several ungrafted grapevine rootstocks (41B, 1103P, 110R and 140Ru) by Assimakopoulou et al. (2016), as well as in other plant species (Hsieh and Waters, 2016; Sabir et al., 2010; Assimakopoulou et al., 2011), although the mechanisms involved have not been described, but should be addressed in future studies. Manganese plays a role in plant metabolism, particularly chlorophyll biosynthesis, water photolysis and enzyme activation (Alejandro et al., 2020), while P is vital for plant growth and productivity as it play roles in phospholipid biosynthesis, photosynthesis, energy transfer, and sugar metabolism

(Malhotra et al., 2018). Therefore, the decrease in their concentration under Fe deficiency conditions could further be a factor in the limitation of plant growth and loss of young leaf chlorophyll (Ceballos-Laita et al., 2022; Nam et al., 2021; Meng et al., 2021) and both of these nutrients are less available at high pH values, further confirming the pH effect of bicarbonate.

4.2. Mitigation of Fe deficiency stress in tolerant rootstocks by remodeling root growth

Under Fe deficiency the increases in root surface area may facilitate Fe uptake by (i) mining larger soil volume (Li et al., 2016), (ii) providing more active sites for FCR activity (Jin et al., 2008), and (iii) lowering rhizosphere pH and releasing of Fe chelators through the increased root exudation which improve Fe solubility (Ma et al., 2022). The tolerant rootstock Fercal strongly induced root growth under bicarbonate stress in contrast to 3309C and treatment with −Fe (Fig. 2B, Table 2), indicating the importance of root system branching as an adaptive response to maintain adequate Fe levels under Fe deficiency conditions (Assimakopoulou et al., 2016). The growth could be facilitated by auxin with the auxin-responsive gene family *Small Auxin Upregulated RNAs* (SAURs) as regulators of plant growth and responses to various stresses (He et al., 2021). Indeed, the expression of two *Small Auxin Upregulated RNAs* (*VviSAUR* and *VviSAUR66*) genes were highly induced in Fercal under both Fe deficiency conditions, while induction was observed only under bicarbonate stress in 3309C. Additionally, *VviZAT6* was enhanced expressed and may have contributed to the growth promotion, as this group of C2H2-type zinc finger proteins has an important role in altering the architecture of the root system by increasing the number and length of lateral roots (Han et al., 2020) and regulating root morphology under nutrient-deficient conditions (Devaiah et al., 2007; Liu et al., 2014). Taken together, we could show, that tolerant plants can activate several mechanisms to promote root biomass, that contribute to their adaptation to limited Fe availability.

4.3. Enhanced organic acids accumulation as a key factor for efficient Fe acquisition under bicarbonate stress

The accumulation of organic acids in plant roots is a common response to Fe deficiency stress, especially in the presence of bicarbonate (Shi et al., 2022; Tato et al., 2020; Sánchez-Rodríguez et al., 2014) and has been shown also for grapevine (Covarrubias and Rombolà, 2015; López-Rayo et al., 2015). These results are consistent with those of (Ollat et al., 2003), who reported an increase in citric and malic acid in Fercal roots grown under iron-deficient conditions and confirmed in other grapevine chlorosis-tolerant genotypes, such as 140R (Covarrubias and Rombolà, 2013) and hybrids of Vitis vinifera and Vitis berlandieri (Brancadoro et al., 1995). Our results hint towards stress and genotype-specific responses. Under bicarbonate stress, increased malic acid in 3309C and Fercal root tips suggests a general adaptation linked to elevated PEPC and PEPCK expression (Fig. 7). While in exudation, the susceptible rootstock 3309C was not able to enhance malic acid exudation under bicarbonate stress, which was the case for Fercal. An increase in citrate and malate under Fe starvation has been observed in grapevine in both root tissue and exudate, possibly acting as primary carboxylates (Covarrubias and Rombolà, 2015; Martínez-Cuenca et al., 2013a). Phosphoenolpyruvate carboxylase catalyzes the addition of bi carbonate (HCO_3^-) to phosphoenolpyruvate, and is a key enzyme actively involved in primary metabolism, pH homeostasis, and organic acids biosynthesis in cells (Rojas et al., 2019). Fe-limited conditions, particularly high bicarbonate levels, enhance PEPC enzyme activity, leading to an increased accumulation of organic acids in the roots (Covarrubias et al., 2016; Andaluz et al., 2002). Although *PHOSPHOENOLPYRUVATE CARBOXILASE 3* (*VviPEPC3*) gene was not significantly induced in either rootstock under either Fe deficiency condition, *VviPPCK1*, which activates PEPC by phosphorylation, was upregulated under +Fe+BIC treatment, suggesting increased activity of PEPC to alleviate the pH variation induced by bicarbonate (Gregory et al., 2009). Bicarbonate stress also triggered increased malate accumulation in root tips and upregulated TCA cycle genes, particularly those producing NADH, such as α-ketoglutarate dehydrogenase and malate dehydrogenase. This suggests a distinct response to bicarbonate-induced Fe deficiency in grapevine roots. The induced activity of the TCA cycle seems to be a vital part of this response and may be necessary to provide the ATP and reduce power required by the increase in *Strategy I* Fe acquisition responses, i.e. FCR activity, as discussed by López-Millán et al. (2013).

4.4. Iron homeostasis regulation between plant tissues as a key factor for Fe deficiency tolerance in grapevine rootstocks

Iron homeostasis depends on Fe uptake, transport and storage, and our expression results could highlight some genotype-specific differences between susceptible and tolerant rootstocks. In this experiment, FCR enzyme activity was reduced in 3309C under both applied stresses, whereas no change was observed in the root tips of Fercal. Previous studies have reported increased FCR activity in tolerant grapevine rootstocks, such as 140R, which demonstrated a high capacity to increase Fe reduction capacity when grown under Fe-limited conditions (Bavaresco et al., 1991; Marastoni et al., 2020). Surprisingly, *VviFRO2* gene expression increased in Fercal under both Fe deficiency conditions, while 3309C showed only a slight increase in expression under +Fe+BIC treatment. However, these transcriptional differences did not correspond directly to changes in FCR enzyme activity, maybe due to the occurrence oof different reductase isoforms that contribute to the cumulative physiological enzymatic activity. It is worth noting that the increased root system observed under +Fe+BIC treatment could also influence FCR activity calculations. Iron transport from soil into root cells is facilitated by the *IRT1* transporter, and its upregulation, along with FRO2, is a well-known marker of Fe deficiency as indicated in the "ferrome" study (Schmidt and Buckhout, 2011) and previous research on plants, including grapevine (Vert et al., 2002; Zamboni et al., 2012; Krausko et al., 2021; Vannozzi et al., 2017). Interestingly, the expression of *VviIRT1* was strongly enhanced in the susceptible rootstock 3309C under both stress conditions, but specifically under bicarbonate stress. This induction was much higher than the values obtained for the tolerant rootstock Fercal. In agreement with the "ferrome" and with the extensive literature of the last decade (for a review see Vélez-Bermúdez and Schmidts, 2023), our data showed the enhanced expression of two bHLH genes (*VvibHLH38* and *VvibHLH38/39*) in both rootstocks and under both conditions of Fe deficiency. Similarly, Vannozzi et al. (2017) demonstrated an enhanced expression of *VvibHLH38* gene in both tolerant (M1) and susceptible (101.14) grapevine rootstocks. This evidence supports the conclusion that even in grapevine the upregulation of *VviIRT1, VviFRO2* and *VviAHA2* can be due transcriptional regulation by bHLHs although the transcriptional and functional level of individual genes needs further clarification.

Upon Fe uptake, Fe needs to be translocated within the plant to the sites of demand. Genes such as *OPT3, IREG3,* and *ZIF1* have been reported to increase expression to maintain Fe content in different organs in a steady state (García et al., 2018; Wang et al., 2019; Lee et al., 2021). Similarly, our results revealed increased expression of these genes in both rootstocks under both Fe deficiency treatments, with Fercal showing slightly higher expression levels under bicarbonate stress. The expression of the gene *VviVIT1* appeared to be inhibited by bicarbonate stress, resulting in decreased expression in both rootstocks. Among the most strongly induced genes were *VviNRAMP6* and *VviFRD3*, and interestingly their expression levels were slightly affected by the interaction between the stress type and grapevine genotype. Several members of the *NRAMP* protein family are participating in the regulation of various metal homeostasis (e.g., Fe and Mn) under their deficient conditions (Ishida et al., 2018). The *FRD3* gene, which belongs to the *MATE* family, encodes an important transporter required for the Fe(III) citrate

complex transport in xylem sap and Fe translocation to the shoot (Wu et al., 2018) and the *YSL* (*Yellow Stripe-Like*) genes encode transporters involved in the transport and translocation of Fe^{3+}-complexes within the plant, particularly the *YSL6* gene which has been reported to have a role in the transport of the Fe(II)-nicotianamine complex (Divol et al., 2013). In our study, the expression *of VviFRD3* gene increased under both Fe deficiency conditions in both rootstocks (higher in Fercal, especially under −Fe treatment), while the *VviYSL6* gene showed higher expression under bicarbonate stress in Fercal compared to 3309C.

A hypothesis could be that both rootstocks under −Fe treatment were able to translocate Fe towards young leaves, as supported by the Fe distribution as a percentage between different plant organs based on the Fe concentrations determined in roots and leaves (Fig. 4D). However, only the tolerant rootstock (Fercal) was able to translocate Fe to the young leaves under +Fe+BIC treatment similar to the −Fe condition, while this was not possible for the susceptible rootstock (3309C).

5. Conclusion

Our research highlights distinct response mechanisms to Fe deficiency in grapevine rootstocks, influenced by the cause of low Fe availability. Rootstock tolerance to Fe deficiency-induced chlorosis depends on their ability to meet Fe demand under environmental stresses that limit Fe availability. 3309C plants showed higher Fe concentrations, indicating higher Fe demand, but demonstrated lower adaptive capacity under Fe deficiency conditions. Responses to Fe deficiency caused by low Fe availability differed from those caused by high bicarbonate levels in several aspects, including the underlying physiological and molecular mechanisms. The tolerant genotype (Fercal) efficiently delivered Fe to young leaves, maintaining higher chlorophyll levels and reducing chlorosis under bicarbonate stress. Fercal also showed higher Fe acquisition efficiency by adapting gene expression related to Fe uptake, transport, and translocation, and increasing the activity of the corresponding enzymes in their roots (e.g., FCR, PEPC, FRD).

Funding

This work was funded in whole or in part by the Austrian Science Fund (FWF) as a part of the VineLresp project (P 32986-B, Grant DOI: 10.55776/P329G) and further supported by a grant (SI 25/2023) provided by the Austria ‘s Agency for Education and Internationalisation (OeAD-GmbH and by a grant number (BI-AT/23-24-005) provided by the Slovenian Research and Innovation Agency in the framework of the Scientific and Technological Cooperation between Austria and Slovenia. Open access funding provided by University of Natural Resources and Life Sciences Vienna (BOKU). For open access purposes, the author has applied a CC BY public copyright license to any author-accepted manuscript version arising from this submission.

Data availability statement

RNA-Seq data are available at NCBI sequence read archive (SRA) with BioProject accession number PRJNA1122387 (https://www.ncbi.nlm.nih.gov/sra/PRJNA1122387). Metadata and all measured raw data are deposited at the Zenodo repository of the University of Natural Resources and Life Sciences, Vienna, and should be cited as Griesser, M., & Khalil, S. (2024). Plant measurements and analytical results of direct and induced iron deficiency of grapevine rootstocks. Zenodo. 10.5281/zenodo.11368046.

Additional files

Table S1. Mineral element concentrations of the root, young leaves (yL), and old leaves (oL) of two grapevine rootstocks, 3309C, and Fercal, grown in different iron availability conditions: control (+Fe), direct Fe deficiency (−Fe), and induced Fe deficiency (+Fe+BIC).

Table S2. Detailed statistics for the quality of sequencing data

Table S3. The top enriched Gene Ontology terms of Molecular Function (MF) related to DEGs (differentially expressed genes) for Fercal and 3309C in the no Fe available vs control (−Fe vs +Fe) comparison ($|\log2\ FC| \geq 1$, FDR < 0.05).

Table S4. The top enriched Gene Ontology terms of Molecular Function (MF) related to DEGs (differentially expressed genes) for Fercal and 3309C in the bicarbonate stress vs control (+Fe+BIC vs +Fe) comparison ($|\log2\ FC| \geq 1$, FDR < 0.05).

Table S5. The top enriched Gene Ontology terms of Biological Process (BP) related to DEGs (differentially expressed genes) for Fercal and 3309C in the no Fe available vs control (−Fe vs +Fe) comparison ($|\log2\ FC| \geq 1$, FDR < 0.05).

Table S6. The top enriched Gene Ontology terms of Biological Process (BP) related to DEGs (differentially expressed genes) for Fercal and 3309C in the bicarbonate stress vs control (+Fe+BIC vs +Fe) comparison ($|\log2\ FC| \geq 1$, FDR < 0.05).

Table S7. The common up-regulated DEGs (differentially expressed genes) and their functions between (-Fe vs +Fe) and (+Fe+BIC vs +Fe) comparisons in Fercal ($|\log2\ FC| \geq 1$, FDR < 0.05) (shown in Venn diagram Fig 5A).

Table S8. The common down-regulated DEGs (differentially expressed genes) and their functions between (-Fe vs +Fe) and (+Fe+BIC vs +Fe) comparisons in Fercal ($|\log2\ FC| \geq 1$, FDR < 0.05) (shown in Venn diagram Fig 5A).

Table S9. The common up-regulated DEGs (differentially expressed genes) and their functions between (-Fe vs +Fe) and (+Fe+BIC vs +Fe) comparisons in 3309C ($|\log2\ FC| \geq 1$, FDR < 0.05) (shown in Venn diagram Fig 5A).

Table S10. The common down-regulated DEGs (differentially expressed genes) and their functions between (-Fe vs +Fe), and (+Fe+BIC vs +Fe) comparisons in 3309C ($|\log2\ FC| \geq 1$, FDR < 0.05) (shown in Venn diagram Fig 5A).

Table S11. Common and Uncommon gene responses involved in Fe uptake, Fe transport, Fe storage and root development in grapevine rootstocks (Fercal,3309C) under Fe deficiency conditions compared to the known "ferrome".

CRediT authorship contribution statement

Sarhan Khalil: Writing – original draft, Data curation. **Rebeka Strah:** Writing – review & editing. **Arianna Lodovici:** Writing – review & editing. **Petr Vojta:** Software. **Jörg Ziegler:** Writing – review & editing. **Maruša Pompe Novak:** Writing – review & editing. **Laura Zanin:** Writing – review & editing. **Nicola Tomasi:** Writing – review & editing. **Astrid Forneck:** Writing – review & editing, Supervision. **Michaela Griesser:** Writing – original draft, Supervision.

Declaration of competing interest

The authors declare that they have no known competing financial interests or personal relationships that could have appeared to influence the work reported in this paper.

Supplementary materials

Supplementary material associated with this article can be found, in the online version, at doi:10.1016/j.stress.2025.100841.

References

Abadía, J., 1992. Leaf responses to Fe deficiency: a review. J. Plant Nutr. 15 (10), 1699–1713.
Abadía, J., López-Millán, A.F., Rombolà, A., Abadía, A., 2002. Organic acids and Fe deficiency: a review. Plant Soil 241, 75–86.
Adeleke, R., Nwangburuka, C., Oboirien, B., 2017. Origins, roles and fate of organic acids in soils: a review. South Afr. J. Bot. 108, 393–406.

Al-Mansouri, H., Alhendawi, R., 2014. Effect of Increasing Concentration of Bicarbonate on Plant Growth and Nutrient Uptake by Maize Plants.
Alejandro, S., Höller, S., Meier, B., Peiter, E., 2020. Manganese in plants: from acquisition to subcellular allocation. Front. Plant Sci. 11, 517877.
Andaluz, S., López-Millán, A.F., Peleato, M.L., Abadía, J., Abadía, A., 2002. Increases in phospho enol pyruvate carboxylase activity in iron-deficient sugar beet roots: analysis of spatial localization and post-translational modification. Plant Soil 241, 43–48.
Asins, M.J., Raga, M.V., Roca, D., Carbonell, E.A., 2020. QTL and candidate gene analyses of rootstock-mediated mandarin fruit yield and quality traits under contrasting iron availabilities. Tree Genet. Genomes 16, 1–15.
Assimakopoulou, A., Holevas, C.D., Fasseas, K., 2011. Relative susceptibility of some Prunus rootstocks in hydroponics to iron deficiency. J. Plant Nutr. 34 (7), 1014–1033.
Assimakopoulou, A., Nifakos, K., Kalogeropoulos, P., Salmas, I., Agelopoulos, K., 2016. Response of ungrafted rootstocks and rootstocks grafted with wine grape varieties (Vitis sp.) to 'lime-induced chlorosis. J. Plant Nutr. 39 (1), 71–86.
Atencio, L., Salazar, J., Lauter, A.N.M., Gonzales, M.D., O'Rourke, J.A., Graham, M.A., 2021. Characterizing short and long term iron stress responses in iron deficiency tolerant and susceptible soybean (Glycine max L. Merr.). Plant Stress 2, 100012.
Aung, M.S., Masuda, H., Kobayashi, T., Nishizawa, N.K., 2018. Physiological and transcriptomic analysis of responses to different levels of iron excess stress in various rice tissues. Soil Sci. Plant Nutr. 64 (3), 370–385.
Bavaresco, L., Fregoni, M., Fraschini, P., 1991. Investigations on iron uptake and reduction by excised roots of different grapevine rootstocks and a V. vinifera cultivar. Plant Soil. 130, 109–113.
Bavaresco, L., Fregoni, H., Fraschini, P., 1992. Investigations on some physiological parameters involved in chlorosis occurrence in grafted grapevine. J. Plant Nutr. 15 (10), 1791–1807.
Bavaresco, L., Fregoni, M., Perino, A., 1994. Physiological aspects of lime-induced chlorosis in some Vitis species. I. Pot trial on calcareous soil. Vitis 33 (2), 123–126.
Bavaresco, L., Giachino, E., Colla, R., 1999. Iron chlorosis paradox in grapevine. J. Plant Nutr. 22 (10), 1589–1597.
Belkhodja, R., Morales, F., Sanz, M., Abadía, A., Abadía, J., 1998. Iron deficiency in peach trees: effects on leaf chlorophyll and nutrient concentrations in flowers and leaves. Plant Soil 203, 257–268.
Bertamini, M., Nedunchezhian, N., Borghi, B., 2001. Effect of iron deficiency induced changes on photosynthetic pigments, ribulose-1, 5-bisphosphate carboxylase, and photosystem activities in field grown grapevine (Vitis vinifera L. cv. Pinot noir) leaves. Photosynthetica 39, 59–65.
Bertamini, M., Nedunchezhian, N., 2005. Grapevine growth and physiological responses to iron deficiency. J. Plant Nutr. 28 (5), 737–749.
Bonnot, T., Gillard, M.B., Nagel, D.H., 2019. A simple protocol for informative visualization of enriched gene ontology terms. Bio Protoc. e3429. -e3429.
Brancadoro, L., Rabotti, G., Scienza, A., Zocchi, G., 1995. Mechanisms of Fe-efficiency in roots of Vitis spp. in response to iron deficiency stress. Plant Soil 171, 229–234.
Ceballos-Laita, L., Takahashi, D., Uemura, M., Abadía, J., López-Millán, A.F., Rodríguez-Celma, J., 2022. Effects of Fe and Mn deficiencies on the root protein profiles of tomato (Solanum lycopersicum) using two-dimensional electrophoresis and Label-Free shotgun analyses. Int. J. Mol. Sci. 23 (7), 3719.
Challam, C., Dutt, S., Sudhakar, D., Raveendran, M., Buckseth, T., Singh, R.K., 2021. Increase in root branching enhanced ferric-chelate reductase activity under iron stress in potato (Solanum tuberosum). Indian J. Agric. Sci. 91 (11), 1646–1649.
Chen, Y., Barak, P., 1982. Iron nutrition of plants in calcareous soils. Adv. Agronomy 35, 217–240.
Chen, Y.T., Wang, Y., Yeh, K.C., 2017. Role of root exudates in metal acquisition and tolerance. Curr. Opin. Plant Biol. 39, 66–72.
Chutia, R., Scharfenberg, S., Neumann, S., Abel, S., Ziegler, J., 2021. Modulation of phosphate deficiency-induced metabolic changes by iron availability in Arabidopsis thaliana. Int. J. Mol. Sci. 22 (14), 7609.
Covarrubias, J.I., Retamales, C., Donnini, S., Rombolà, A.D., Pastenes, C., 2016. Contrasting physiological responses to iron deficiency in Cabernet Sauvignon grapevines grafted on two rootstocks. Sci. Hortic. 199, 1–8.
Covarrubias, J.I., Rombolà, A.D., 2013. Physiological and biochemical responses of the iron chlorosis tolerant grapevine rootstock 140 Ruggeri to iron deficiency and bicarbonate. Plant Soil. 370 (1), 305–315. https://doi.org/10.1007/s11104-013-1623-2.
Covarrubias, J.I., Rombolà, A.D., 2015. Organic acids metabolism in roots of grapevine rootstocks under severe iron deficiency. Plant Soil. 394 (1), 165–175. https://doi.org/10.1007/s11104-015-2530-5.
Devaiah, B.N., Nagarajan, V.K., Raghothama, K.G., 2007. Phosphate Homeostasis and Root Development in Arabidopsis are Synchronized by the Zinc Finger.
Divol, F., Couch, D., Conéjéro, G., Roschzttardtz, H., Mari, S., Curie, C., 2013. The Arabidopsis YELLOW STRIPE LIKE4 and 6 transporters control iron release from the chloroplast. Plant Cell 25 (3), 1040–1055.
Dobin, A., Davis, C.A., Schlesinger, F., Drenkow, J., Zaleski, C., Jha, S., Batut, P., Chaisson, M., Gingeras, T.R., 2013. STAR: ultrafast universal RNA-seq aligner. Bioinformatics 29 (1), 15–21.
Donnini, S., Castagna, A., Ranieri, A., Zocchi, G., 2009. Differential responses in pear and quince genotypes induced by Fe deficiency and bicarbonate. J. Plant Physiol. 166 (11), 1181–1193.
Eide, D., Broderius, M., Fett, J., Guerinot, M.L., 1996. A novel iron-regulated metal transporter from plants identified by functional expression in yeast. Proc. Natl. Acad. Sci. 93 (11), 5624–5628.
El Amine, B., Mosseddaq, F., Naciri, R., Oukarroum, A., 2023. Interactive effect of Fe and Mn deficiencies on physiological, biochemical, nutritional and growth status of Soybean. Plant Physiol. Biochem. 199, 107718.
Ewels, P., Magnusson, M., Lundin, S., Käller, M., 2016. MultiQC: summarize analysis results for multiple tools and samples in a single report. Bioinformatics 32 (19), 3047–3048.
Fu, L., Zhu, Q., Sun, Y., Du, W., Pan, Z., Sa, Peng, 2017. Physiological and transcriptional changes of three citrus rootstock seedlings under iron deficiency. Front. Plant Sci. 8, 1104.
Gao, F., Robe, K., Gaymard, F., Izquierdo, E., Dubos, C., 2019. The transcriptional control of iron homeostasis in plants: a tale of bHLH transcription factors? Front. Plant Sci. 10, 6.
García, M.J., Corpas, F.J., Lucena, C., Alcántara, E., Pérez-Vicente, R., Zamarreño, Á.M., Bacaicoa, E., García-Mina, J.M., Bauer, P., Romera, F.J., 2018. A shoot Fe signaling pathway requiring the OPT3 transporter controls GSNO reductase and ethylene in Arabidopsis thaliana roots. Front. Plant Sci. 9, 375982.
Ge, S.X., Son, E.W., Yao, R., 2018. iDEP: an integrated web application for differential expression and pathway analysis of RNA-Seq data. BMC Bioinformatics 19, 1–24.
Götz, S., García-Gómez, J.M., Terol, J., Williams, T.D., Nagaraj, S.H., Nueda, M.J., Robles, M., Talón, M., Dopazo, J., Conesa, A., 2008. High-throughput functional annotation and data mining with the Blast2GO suite. Nucleic Acids Res. 36 (10), 3420–3435.
Gregory, A.L., Hurley, B.A., Tran, H.T., Valentine, A.J., She, Y.-M., Knowles, V.L., Plaxton, W.C., 2009. In vivo regulatory phosphorylation of the phosphoenolpyruvate carboxylase AtPPC1 in phosphate-starved Arabidopsis thaliana. Biochem. J. 420 (1), 57–65.
Han, G., Wei, X., Dong, X., Wang, C., Sui, N., Guo, J., Yuan, F., Gong, Z., Li, X., Zhang, Y., 2020. Arabidopsis ZINC FINGER PROTEIN1 acts downstream of GL2 to repress root hair initiation and elongation by directly suppressing bHLH genes. Plant Cell 32 (1), 206–225.
He, Y., Liu, Y., Li, M., Lamin-Samu, A.T., Yang, D., Yu, X., Izhar, M., Jan, I., Ali, M., Lu, G., 2021. The Arabidopsis SMALL AUXIN UP RNA32 protein regulates ABA-mediated responses to drought stress. Front. Plant Sci. 12, 625493.
Hiscox, J., Israelstam, G., 1979. A method for the extraction of chlorophyll from leaf tissue without maceration. Canadian J. Bot. 57 (12), 1332–1334.
Hoagland, D.R., Arnon, D.I., 1950. The water-culture method for growing plants without soil. Circular California Agricultural Experiment Station 347, 2nd edit.
Hsieh, E.J., Waters, B.M., 2016. Alkaline stress and iron deficiency regulate iron uptake and riboflavin synthesis gene expression differently in root and leaf tissue: implications for iron deficiency chlorosis. J. Exp. Bot. 67 (19), 5671–5685.
Ishida, J.K., Caldas, D.G., Oliveira, L.R., Frederici, G.C., Leite, L.M.P., Mui, T.S., 2018. Genome-wide characterization of the NRAMP gene family in Phaseolus vulgaris provides insights into functional implications during common bean development. Genet. Mol. Biol. 41, 820–833.
Ivanov, R., Brumbarova, T., Bauer, P., 2012. Fitting into the harsh reality: regulation of iron-deficiency responses in dicotyledonous plants. Mol. Plant 5 (1), 27–42.
Jin, C.W., Chen, W.W., Meng, Z.B., Zheng, S.J., 2008. Iron deficiency-induced increase of root branching contributes to the enhanced root ferric chelate reductase activity. J. Integr. Plant Biol. 50 (12), 1557–1562.
Justi, M., Silva, C.A., Rosa, S.D., 2022. Organic acids as complexing agents for iron and their effects on the nutrition and growth of maize and soybean. Arch. Agronomy Soil Sci. 68 (10), 1369–1384.
Karimi, R., Salimi, F., 2021. Iron-chlorosis tolerance screening of 12 commercial grapevine (Vitis vinifera L.) cultivars based on phytochemical indices. Sci. Hortic. 283, 110111.
Khalil, S., Strah, R., Lodovici, A., Vojta, P., Berardinis, F.D., Ziegler, J., Novak, M.P., Zanin, L., Tomasi, N., Forneck, A., 2024. The activation of iron deficiency responses of grapevine rootstocks is dependent to the availability of the nitrogen forms. BMC Plant Biol. 24 (1), 218.
Kim, S.A., LaCroix, I.S., Gerber, S.A., Guerinot, M.L., 2019. The iron deficiency response in Arabidopsis thaliana requires the phosphorylated transcription factor URI. Proc. Natl. Acad. Sci. 116 (50), 24933–24942.
Kobayashi, T., Nozoye, T., Nishizawa, N.K., 2019. Iron transport and its regulation in plants. Free Radic. Biol. Med. 133, 11–20.
Krausko, M., Labajová, M., Peterková, D., Jásik, J., 2021. Specific expression of AtIRT1 in phloem companion cells suggests its role in iron translocation in aboveground plant organs. Plant Signal. Behav. 16 (9), 1925020.
Ksouri, R., M'rah, S., Gharsalli, M., Lachaâl, M., 2006. Biochemical responses to true and bicarbonate-induced iron deficiency in grapevine genotypes. J. Plant Nutr. 29 (2), 305–315.
Lampreave, M., Mateos, A., Valls, J., Nadal, M., Sánchez-Ortiz, A., 2022. Carbonated irrigation assessment of grapevine growth, nutrient absorption, and sugar accumulation in a Tempranillo (Vitis vinifera L.) Vineyard. Agriculture 12 (6), 792.
Lee, S., Ricachenevsky, F.K., Punshon, T., 2021. Functional overlap of two major facilitator superfamily transporter, ZIF1, and ZIFL1 in zinc and iron homeostasis. Biochem. Biophys. Res. Commun. 560, 7–13.
Li, G., Kronzucker, H.J., Shi, W., 2016. The response of the root apex in plant adaptation to iron heterogeneity in soil. Front. Plant Sci. 7, 181664.
Li, Y., Wang, N., Zhao, F., Song, X., Yin, Z., Huang, R., Zhang, C., 2014. Changes in the transcriptomic profiles of maize roots in response to iron-deficiency stress. Plant Mol. Biol. 85, 349–363.
Liang, G., 2022. Iron uptake, signaling, and sensing in plants. Plant Commun. 3 (5).
Liao, Y., Smyth, G.K., Shi, W., 2014. featureCounts: an efficient general purpose program for assigning sequence reads to genomic features. Bioinformatics 30 (7), 923–930.

Liu, X.-M., An, J., Han, H.J., Kim, S.H., Lim, C.O., Yun, D-J, Chung, W.S., 2014. ZAT11, a zinc finger transcription factor, is a negative regulator of nickel ion tolerance in Arabidopsis. Plant Cell Rep. 33, 2015–2021.
López-Millán, A.F., Grusak, M.A., Abadía, A., Abadía, J., 2013. Iron deficiency in plants: an insight from proteomic approaches. Front. Plant Sci. 4, 254.
López-Rayo, S., Di Foggia, M., Moreira, E.R., Donnini, S., Bombai, G., Filippini, G., Pisi, A., Rombolà, A.D., 2015. Physiological responses in roots of the grapevine rootstock 140 Ruggeri subjected to Fe deficiency and Fe-heme nutrition. Plant Physiol. Biochem. 96, 171–179.
Love, M., Anders, S., Huber, W., 2014. Differential analysis of count data–the DESeq2 package. Genome Biol. 15 (550), 10–1186.
Lucena, C., Romera, F.J., Rojas, C.L., García, M.J., Alcántara, E., Pérez-Vicente, R., 2007. Bicarbonate blocks the expression of several genes involved in the physiological responses to Fe deficiency of Strategy I plants. Funct. Plant Biol. 34 (11), 1002–1009.
Ma, W., Tang, S., Dengzeng, Z., Zhang, D., Zhang, T., Ma, X., 2022. Root exudates contribute to belowground ecosystem hotspots: a review. Front. Microbiol. 13, 937940.
Malhotra, H., Vandana, Sharma S, Pandey, R., 2018. Phosphorus nutrition: plant growth in response to deficiency and excess. Plant Nutr. Abiotic Stress Tolerance 171–190.
Marastoni, L., Lucini, L., Miras-Moreno, B., Trevisan, M., Sega, D., Zamboni, A., Varanini, Z., 2020. Changes in physiological activities and root exudation profile of two grapevine rootstocks reveal common and specific strategies for Fe acquisition. Sci. Rep. 10 (1), 18839.
Martínez-Cuenca, M.R., Iglesias, D.J., Talón, M., Abadía, J., López-Millán, A.F., Primo-Millo, E., Legaz, F., 2013a. Metabolic responses to iron deficiency in roots of Carrizo citrange [Citrus sinensis (L.) Osbeck.× Poncirus trifoliata (L.) Raf.]. Tree Physiol. 33 (3), 320–329.
Martínez-Cuenca, M.R., Legaz, F., Forner-Giner, M.Á., Primo-Millo, E., Iglesias, D.J., 2013b. Bicarbonate blocks iron translocation from cotyledons inducing iron stress responses in Citrus roots. J. Plant Physiol. 170 (10), 899–905.
Masuda, H., Aung, M.S., Maeda, K., Kobayashi, T., Takata, N., Taniguchi, T., Nishizawa, N.K., 2018. Iron-deficiency response and expression of genes related to iron homeostasis in poplars. Soil Sci. Plant Nutr. 64 (5), 576–588.
Meng, X., Chen, W.W., Wang, Y.Y., Huang, Z.R., Ye, X., Chen, L.S., Yang, L.T., 2021. Effects of phosphorus deficiency on the absorption of mineral nutrients, photosynthetic system performance and antioxidant metabolism in Citrus grandis. PLoS One 16 (2), e0246944.
Młodzińska-Michta, E., 2023. Abiotic factors determine the root system architecture – review and update. Acta Societatis Botanicorum Poloniae 92 (1). https://doi.org/10.5586/asbp/168700.
Molassiotis, A.N., Diamantidis, G.C., Therios, I.N., Tsirakoglou, V., Dimassi, K.N., 2005. Oxidative stress, antioxidant activity and Fe (III)-chelate reductase activity of five Prunus rootstocks explants in response to Fe deficiency. Plant Growth Regul. 46, 69–78.
Molnár, Z., Solomon, W., Mutum, L., Janda, T., 2023. Understanding the mechanisms of Fe deficiency in the rhizosphere to promote plant resilience. Plants 12 (10), 1945.
Nam, H.I., Shahzad, Z., Dorone, Y., Clowez, S., Zhao, K., Bouain, N., Lay-Pruitt, K.S., Cho, H., Rhee, S.Y., Rouached, H., 2021. Interdependent iron and phosphorus availability controls photosynthesis through retrograde signaling. Nat. Commun. 12 (1), 7211.
Okonechnikov K., Conesa A., Qualimap F.G.A. (2016) Qualimap2: advanced multi-sample quality control for high-throughput sequencing data., 2016, 32. DOI: https://doi.org/10.1093/bioinformatics/btv566 PMID: https://www.ncbi.nlm.nih.gov/pubmed/26428292:292-294.
Ollat, N., Laborde, B., Neveux, M., Diakou-Verdin, P., Renaud, C., Moing, A., 2003. Organic acid metabolism in roots of various grapevine (Vitis) rootstocks submitted to iron deficiency and bicarbonate nutrition. J. Plant Nutr. 26 (10–11), 2165–2176.
Panchal, P., Miller, A.J., Giri, J., 2021. Organic acids: versatile stress-response roles in plants. J. Exp. Bot. 72 (11), 4038–4052.
Pestana, M., Gama, F., Saavedra, T., De Varennes, A., Correia, P.J., 2012. The root ferric-chelate reductase of Ceratonia siliqua (L.) and Poncirus trifoliata (L.) Raf. responds differently to a low level of iron. Sci. Hortic. 135, 65–67.
Pouget, R., Ottenwaelter, M., 1978. Etude de l'adaptation de nouvelles variétés de porte-greffes à des sols très chlorosants. Conn. Vigne Vin. 12, 167–175.
Robinson, N.J., Procter, C.M., Connolly, E.L., Guerinot, M.L., 1999. A ferric-chelate reductase for iron uptake from soils. Nature 397 (6721), 694–697.
Rojas, B.E., Hartman, M.D., Figueroa, C.M., Leaden, L., Podestá, F.E., Iglesias, A.A., 2019. Biochemical characterization of phospho enol pyruvate carboxykinases from Arabidopsis thaliana. Biochem. J. 476 (20), 2939–2952.
Römheld, V., 2000. The chlorosis paradox: Fe inactivation as a secondary event in chlorotic leaves of grapevine. J. Plant Nutr. 23 (11–12), 1629–1643.
Rout, G.R., Sahoo, S., 2015. Role of iron in plant growth and metabolism. Rev. Agric. Sci. 3, 1–24.
Rustioni, L., Grossi, D., Brancadoro, L., Failla, O., 2017. Characterization of iron deficiency symptoms in grapevine (Vitis spp.) leaves by reflectance spectroscopy. Plant Physiol. Biochem. 118, 342–347.
Sabir, A., Ekbic, H.B., Herdem, H., Tangolar, S., 2010. Response of four grapevine (Vitis spp.) genotypes to direct or bicarbonate-induced iron deficiency. Spanish J. Agric. Res. (3), 823–829.
Saleem, A., Zulfiqar, A., Saleem, M.Z., Ali, B., Saleem, M.H., Ali, S., Tufekci, E.D., Tufekci, A.R., Rahimi, M., Mostafa, R.M., 2023. Alkaline and acidic soil constraints on iron accumulation by Rice cultivars in relation to several physio-biochemical parameters. BMC Plant Biol. 23 (1), 397.
Sánchez-Rodríguez, A., Del Campillo, M., Torrent, J., Jones, D., 2014. Organic acids alleviate iron chlorosis in chickpea grown on two p-fertilized soils. J. Soil. Sci. Plant Nutr. 14 (2), 292–303.
Santangeli, M., Steininger-Mairinger, T., Vetterlein, D., Hann, S., Oburger, E., 2024. Maize (Zea mays L.) root exudation profiles change in quality and quantity during plant development–a field study. Plant Sci. 338, 111896.
Santi, S., Schmidt, W., 2009. Dissecting iron deficiency-induced proton extrusion in Arabidopsis roots. New Phytol. 183 (4), 1072–1084.
Savoi, S., Herrera, J.C., Forneck, A., Griesser, M., 2019. Transcriptomics of the grape berry shrivel ripening disorder. Plant Mol. Biol. 100, 285–301.
Schmidt, W., Buckhout, T.J., 2011. A hitchhiker's guide to the Arabidopsis ferrome. Plant Physiol. Biochem. 49 (5), 462–470.
Seifert, E., 2014. OriginPro 9.1: scientific data analysis and graphing software-software review. J. Chem. Inf. Model. 54 (5), 1552.
Shi, Y., Guo, S., Zhao, X., Xu, M., Xu, J., Xing, G., Zhang, Y., Ahammed, G.J., 2022. Comparative physiological and transcriptomics analysis revealed crucial mechanisms of silicon-mediated tolerance to iron deficiency in tomato. Front. Plant Sci. 13, 1094451.
Siminis, C.I., Stavrakakis, M.N., 2008. Iron induces root and leaf ferric chelate reduction activity in grapevine rootstock 140 Ruggeri. HortScience 43 (3), 685–690.
Simons, A., 2010. FastQC: a quality control tool for high throughput sequence data (Online). A Quality Control Tool for High Throughput Sequence Data 10: f1000research. http://www.bioinformatics.babraham.ac.uk/projects/fastqc/.
Sun, S., Li, J., Song, H., Chen, D., Tu, M., Chen, Q., Jiang, G., Zhou, Z., 2022. Comparative transcriptome and physiological analyses reveal key factors in the tolerance of peach rootstocks to iron deficiency chlorosis. 3 Biotech. 12 (1), 38.
Tagliavini, M., Rombolà, A.D., 2001. Iron deficiency and chlorosis in orchard and vineyard ecosystems. Eur. J. Agronomy 15 (2), 71–92.
Tato, L., Islam, M., Mimmo, T., Zocchi, G., Vigani, G., 2020. Temporal responses to direct and induced iron deficiency in Parietaria judaica. Agronomy 10 (7), 1037.
Valipour, M., Baninasab, B., Khoshgoftarmanesh, A.H., Gholami, M., 2020. Oxidative stress and antioxidant responses to direct and bicarbonate-induced iron deficiency in two quince rootstocks. Sci. Hortic. 261, 108933.
Vannozzi, A., Donnini, S., Vigani, G., Corso, M., Valle, G., Vitulo, N., Bonghi, C., Zocchi, G., Lucchin, M., 2017. Transcriptional characterization of a widely-used grapevine rootstock genotype under different iron-limited conditions. Front. Plant Sci. 7, 1994.
Vélez-Bermúdez, I.C., Schmidt, W., 2023. Iron sensing in plants. Front. Plant Sci. 14, 1145510.
Vert, G., Grotz, N., Dédaldéchamp, F., Gaymard, F., Guerinot, M.L., Briat, J.F., Curie, C., 2002. IRT1, an Arabidopsis transporter essential for iron uptake from the soil and for plant growth. Plant Cell 14 (6), 1223–1233.
Wang, M., Kawakami, Y., Bhullar, N.K., 2019. Molecular analysis of iron deficiency response in hexaploid wheat. Front. Sustain. Food Syst. 3, 67.
Wang, Y., Kang, Y., Zhong, M., Zhang, L., Chai, X., Jiang, X., Yang, X., 2022. Effects of iron deficiency stress on plant growth and quality in flowering Chinese cabbage and its adaptive response. Agronomy 12 (4), 875.
Wu, T.Y., Gruissem, W., Bhullar, N.K., 2018. Facilitated citrate-dependent iron translocation increases rice endosperm iron and zinc concentrations. Plant Sci. 270, 13–22.
Yunta, F., Martín, I., Lucena, J.J., Gárate, A., 2013. Iron chelates supplied foliarly improve the iron translocation rate in Tempranillo grapevine. Commun. Soil. Sci. Plant Anal. 44 (1–4), 794–804.
Zamboni, A., Zanin, L., Tomasi, N., Pezzotti, M., Pinton, R., Varanini, Z., Cesco, S., 2012. Genome-wide microarray analysis of tomato roots showed defined responses to iron deficiency. BMC Genomics 13, 1–14.
Zanin, L., Venuti, S., Zamboni, A., Varanini, Z., Tomasi, N., Pinton, R., 2017. Transcriptional and physiological analyses of Fe deficiency response in maize reveal the presence of Strategy I components and Fe/P interactions. BMC Genomics 18, 1–15.